



Detailed simulation of storage hydropower systems in large Alpine watersheds

Andrea Galletti, Diego Avesani, Alberto Bellin, Bruno Majone^{*}

Department of Civil, Environmental and Mechanical Engineering, University of Trento, via Mesiano, 77 38123 Trento, Italy

ARTICLE INFO

This manuscript was handled by Corrado Corradini, Editor-in-Chief, with the assistance of Renato Morbidelli, Associate Editor

Keywords:

Water resources management
Large-scale hydrological modelling
Hydropower production
Reservoir modelling
Hydraulic infrastructures

ABSTRACT

Most mountain catchments worldwide are exploited for hydropower production causing significant alterations of their natural regime. Hydrological and water resources modelling in these catchments is challenging because the alterations of natural streamflow caused by hydropower production are often significant, while capturing their variability in space and time requires critical data concerning the hydraulic infrastructures and their operational schedules. These data are difficult to acquire, thereby hindering the possibility to correctly simulate the complex interaction between the natural hydrological cycle and water uses. To overcome these limitations we propose a framework that relies solely on publicly available data which provides accurate simulation of both streamflow and hydropower production. The proposed framework is illustrated by means of the HYPERstreamHS hydrological model applied to the Adige catchment, a large watershed of the south-eastern Alpine region whose streamflow is strongly impacted by 39 large hydropower systems, 22 of which connected to storage reservoirs, with an overall mean annual production that accounts for about 14% of the total Italian hydropower production. We analyzed the impact on modelled hydropower production of commonly adopted simplifications in the production schedule as well as of the hydropower systems, which are often characterized by a complex infrastructure with several interlinked derivations and conveyance intakes. Our simulations highlight how an accurate topological representation of hydraulic infrastructures is crucial to correctly represent water transfers, more important than capturing the operational schedules when reservoir oscillations are a small fraction of the total head. On the contrary, scheduling is important for systems in which reservoir oscillations account for a significant portion of the total head. Furthermore, we show that simplifications motivated by difficulties in data collection combine in a non-linear manner with an overall impact difficult to assess. We propose this framework for accurate modelling of hydropower production at regional and national scales, particularly in studies dealing with the projection of climate change and competing uses on water resources and renewable energy.

1. Introduction

Electricity demand has more than doubled since 1990, and it is expected to increase further in the near future due to population growth (UN, 2019) and to the progressive decarbonization of transportation, housing and energy-intensive industrial sectors (IEA, 2018). Hydropower is an important energy source satisfying more than 19% of electricity demand worldwide (IEA, 2018; Akpinar, 2013), with storage reservoir hydropower being the only Renewable Energy Source (RES) that ensures reliable long-term storage capacity (Barton et al., 2004). For these characteristics, hydropower is expected to play an important role in the future evolution of the electricity market, helping to ensure a smooth transition to a green energy economy. The main adverse effect of hydropower is the loss of freshwater ecosystem services, whose

evaluation catalyzed a wealth of attention (see e.g., Simonov et al., 2019; Yu, 2017; Wang et al., 2010). Measures are today available to attenuate these losses (see e.g., Malm Renöfält et al., 2010; Gabbud and Lane, 2016), though scenarios with progressive decommissioning of reservoirs in favor of a more diffuse use of solar and wind energy have been recently envisioned (Waldman et al., 2019). Although less than other RES, hydropower production is uncertain because of the inherent variability of streamflow at multiple temporal and spatial scales. Moreover, climate change is expected to increase this variability and may act in combination with competing uses to modify timing and amount of water volumes available for electricity production (Smajgl et al., 2016; Anghileri et al., 2018; Zhang et al., 2018). These two external effects may be in synergy, in some regions, and in opposition, in others, depending on the local effect of climate change and evolution of

^{*} Corresponding author.

<https://doi.org/10.1016/j.jhydrol.2021.127125>

Received 2 July 2021; Received in revised form 3 October 2021; Accepted 25 October 2021

Available online 6 November 2021

0022-1694/© 2021 The Author(s).

Published by Elsevier B.V. This is an open access article under the CC BY-NC-ND license

(<http://creativecommons.org/licenses/by-nc-nd/4.0/>).

water demand for other uses, or changes of water use policies. In this context, hydrological modelling is a viable tool to project the impact of these foreseen changes on future hydropower production and evaluate the effects of modifications in the management strategies aimed at mitigating the above adverse effects. Indeed, in the last decades hydrological modelling has been applied at regional and larger scales, often involving complex parameterizations, with the objective of representing at high spatio-temporal resolution the interplay between biotic and abiotic processes controlling the dynamics of the Earth's critical zone (see e.g., Sharif et al., 2007; Wada et al., 2016; Zierl and Bugmann, 2005).

However, climate change is not the only driver of change for water resources, as the projected increase of water use for agriculture, energy and other sectors is creating concerns as well (Bieber et al., 2018; Destouni et al., 2013). Indeed, the effects on water resources of climate change and water uses are difficult to disentangle, given that their interaction may give rise to nonlinear effects which analysis requires information on water uses at a level of detail difficult to achieve (Bellin et al., 2016; Mallucci et al., 2019). Hydropower is the dominant water use in mountain regions and its inclusion into hydrological models requires an adequate description of the hydraulic systems and of their interaction with the natural components of the hydrological cycle (Nazemi and Wheeler, 2015; Nazemi and Wheeler, 2015). Operations of run-of-the-river systems are strictly dependent on streamflow timing, while storage hydropower can modulate its activity to minimize the adverse impacts of climate change and maximize revenue. Moreover, modelling climate change impacts and the effects of changes in water demand on storage hydropower systems requires the introduction of operational constraints as well as suitable production schedules for each hydropower system. Unfortunately these data are difficult to acquire because they are often kept confidential by the hydropower companies; in this situation management strategies should be inferred from other sources. In principle, expert knowledge may suggest a suitable functional form of the water used for hydropower production with the parameters calibrated according to a given objective function. However, this approach adds parameters to models that often are already over-parameterized, thereby increasing the computational cost and uncertainty due to equifinality (Beven and Binley, 1992). As a consequence, when a large number of hydropower systems should be modeled, management rules are assumed a priori according to available constraints (i.e. the hydraulic capacity of the hydropower system), and the topology of the hydropower system is often simplified depending on the available information.

Several deterministic approaches have been adopted in the literature to model reservoir operations, such as e.g. hedging curve rules and target volume approach. The first approach provides partitioning factors for satisfying the downstream demand (from agricultural, hydropower and water supply uses) according to prioritization rules set by the water manager (see e.g. Shrestha et al., 2014; Guo et al., 2013; Tu et al., 2003). This approach considers the seasonality of water inflows and might provide good results but a limitation emerges in the definition of the downstream demand, which has to be known for all hydropower systems being modelled, as well as the hedging thresholds and coefficients. The target volume approach is often preferred for its simplicity (see e.g. Fatichi et al., 2015; Finger et al., 2012). In this case, 365 (daily) target volumes are assigned, and turbinized flows are determined as a function of the difference between current and target volumes. The computation of target volumes can either be based on averaged observations if available, otherwise it is based on reservoir dimension and on normalized target volume time series. While the target volume approach represents a valid option where detailed time series are available, the adoption of normalized target volume curves obtained averaging time series of other reservoirs is unable to capture differences in the management of the reservoirs and this inevitably introduces further uncertainty into the modelled hydropower production. Furthermore, a common assumption of several existing contributions is that the hydropower systems operate

always at their maximum capacity when available water volumes exceed those needed for respecting the imposed Minimum Environmental Flows (MEFs), otherwise it is reduced to the quantity needed to guarantee this priority service (Turner et al., 2017; Wagner et al., 2016; Zhao et al., 2016). This relatively parsimonious approach has been shown to perform well at the global scale and suits well large scale impact assessments (see e.g. Turner et al., 2017; Turner et al., 2017), though it provides unrealistic estimation of water releases from the reservoirs, thus affecting environmental health impact assessments related to hydropower activities (Petruzziello et al., 2021; Zhao et al., 2019).

In this context, reliable modelling of hydropower production at the mesoscale requires a description of hydropower systems accurate enough to fully grasp the complex interactions between the hydrological cycle and the other water uses, particularly when the objective is to assess the impact of climate change or to test policies for mitigating conflicts for water uses. Since technical information on such hydraulic infrastructures is often incomplete and difficult to obtain, we developed and tested a modelling approach that relies on publicly available information for identifying reservoir-specific daily operation schemes. The resulting modelling framework was then validated against historical time series of streamflows and hydropower production. Furthermore, we analyzed the impact on modelled hydropower production of simplifications typically adopted in large scale modelling efforts, both concerning the structure of the hydropower system and its management schedule. In particular we considered: i) a simplification in the geometrical configuration of the hydropower systems by assuming the reservoir as the only water source for the connected generation units, thereby neglecting conveyance intakes whether present; and ii) a simplification of the reservoir operation schedules in which the power plants are always operated at their maximum hydraulic capacity, when the required volume is available, and using all the incoming volume larger than the MEF volume, otherwise.

To this end, we applied the HYPERstreamHS hydrological model (Avesani et al., 2021) to the Adige catchment, a large watershed located in the south-eastern portion of the Alps: the catchment offers a complex scenario, though rather common in Alpine regions, in which a detailed model implementation is expected to improve the model's predictive capabilities. Conversely, given the high level of detail available, the effects of simplifications introduced into the model can be tracked down thus allowing the identification of the systems that are prone to be negatively impacted by such simplifications, for example underestimating hydropower production. In this respect, our results provide guidance for applications in situations in which data are available with fewer details.

The work is organized as follows: Section 2 presents an overview of the model components, with particular emphasis on modelling the hydropower systems, followed by the presentation of the data that are necessary to run the model and of the procedure to approximate hydropower production schemes. Section 3 presents an application of the proposed modelling framework to the Adige watershed and Section 4 presents and discusses model performance in reproducing streamflow and hydropower production of the catchment, and then provides a quantitative assessment of the bias introduced under different simplified configurations. Finally, Section 5 presents the main conclusions.

2. Methods

2.1. Modelling framework

In the present work modelling was performed by using HYPERstreamHS, a distributed hydrological model combining hydrological flows with explicit modelling of hydropower-related water uses and transfers (Avesani et al., 2021). In this framework, vertical hydrological fluxes are computed at each macrocell of the computational grid (grid size is set at 5 km in the present work) and the resulting runoff is routed

to the corresponding downstream node by means of the Width Function Instantaneous Unit Hydrograph (WFIUH) method with the assumption of constant stream velocity (see Natural Hydrological Module in Fig. 1). The nodes are selected locations along the river network where the natural streamflow is computed as the sum of streamflow from the upstream nodes and the runoff produced by the interbasin (i.e., the contributing area of intermediate hillslopes, Fig. 1, left panel). In the presence of human infrastructures additional nodes are included and water mass balances are applied with specific constraints depending on node type (see Human Systems Module in Fig. 1, right panel). Communication between the Natural Hydrological and Human Systems modules takes place at the infrastructures nodes. This is exemplified in the central panel of Fig. 1 where the fluxes entering the mass balance equation at a generic node (in this specific case a reservoir) are highlighted. The total incoming streamflow to the reservoir (node 3) is computed as the sum of the streamflow generated by the interbasin between the two upstream nodes (1 and 2) and the reservoir ($Q_{s,3}(t)$) plus the streamflow transferred from the upstream nodes 1 and 2, $Q_{s,1}(t - \tau_{1,3})$ and $Q_{s,2}(t - \tau_{2,3})$, respectively, with $\tau_{1,3}$ and $\tau_{2,3}$ being the transfer times between two upstream nodes and the downstream reservoir node 3. Water mass balance is then computed at the reservoir (see Section 2.1.2 for the details on the mass balances applied to the different node types) and the outflows $Q_{DER,3}(t)$ and $Q_{NAT,3}(t)$ are computed see (Fig. 1 central panel).

2.1.1. Natural Hydrological module

The hydrological component of the model is based on the HYPERstream routing scheme presented in Piccolroaz et al. (2016), which receives the total runoff generated at the level of the macrocells. The precipitation is first spatially aggregated at the macrocell scale (see left panel in Fig. 1), and then used as input in a degree day module for snow-melting and accumulation. The resulting vertical flow is the input of a continuous SCS-CN module, which separates surface runoff from infiltration (Michel et al., 2005). Then, infiltration feeds a non-linear bucket model for soil moisture dynamics (Majone et al., 2010) with the rapid component of return flow and deep infiltration as output. Evapotranspiration, evaluated with the Hargreaves and Samani (1982) model, is added to the water budget equation at this level of the modelling chain. Finally, deep infiltration enters a second linear bucket representing

groundwater and the associated slow component of the return flow. The total resulting runoff is routed to the nearest downstream node by means of a WFIUH method (Rodríguez-Iturbe and Rinaldo, 1997) applied to the network extracted from the DEM of the area (left panel in Fig. 1).

The model requires a total of 12 parameters, which can be calibrated against streamflow observations by either using the Particle Swarm Optimization (PSO) algorithm (Kennedy and Eberhart, 1995), or exploring the hyperparameters space by means of the Latin Hypercube Sampling (LHS) scheme (McKay et al., 1979), which are both embedded in the model. Two objective functions are included: Nash–Sutcliffe (NSE) index, proposed by Nash and Sutcliffe (1970) and the Kling-Gupta Efficiency index (KGE), proposed by Gupta et al. (2009). In a multi-site calibration framework, the global efficiency index is defined as the average of the efficiencies attained at each adopted gauging station. A detailed description of the hydrological kernel can be found in Avesani et al. (2021). Notice that the surface and subsurface flow generation module was already successfully applied in previous studies conducted in Alpine catchments (Piccolroaz et al., 2015; Bellin et al., 2016; Laiti et al., 2018). In addition to its previous features, HYPERstreamHS was coded for parallel computing through the MPI paradigm to take advantage of the almost perfect scalability of the natural hydrological kernel (Avesani et al., 2021).

2.1.2. Human systems module

In HYPERstreamHS hydraulic infrastructures such as reservoirs, water diversions and tailraces, are modelled by adding nodes at the locations where the natural stream network and the engineered systems are connected. At these nodes local water budgets are applied in the respect of the constraints due to the type of use, as for example the hydraulic capacity of the diversion channel.

After water budget is applied, the resulting partitioned flows (see Fig. 1) are routed downstream from the Human Systems module assuming two different celerity values, the first equal to 2m/s for fluxes travelling along transport hydraulic infrastructures, whereas flows along the natural stream network travel with the same celerity adopted for macrocell-node routing, which is one of the 12 model parameters.

Three types of nodes are considered: 1) reservoir, 2) intake and 3) power plant. Connections between these nodes are also taken into account by including elements such as tunnels, diversion channels and

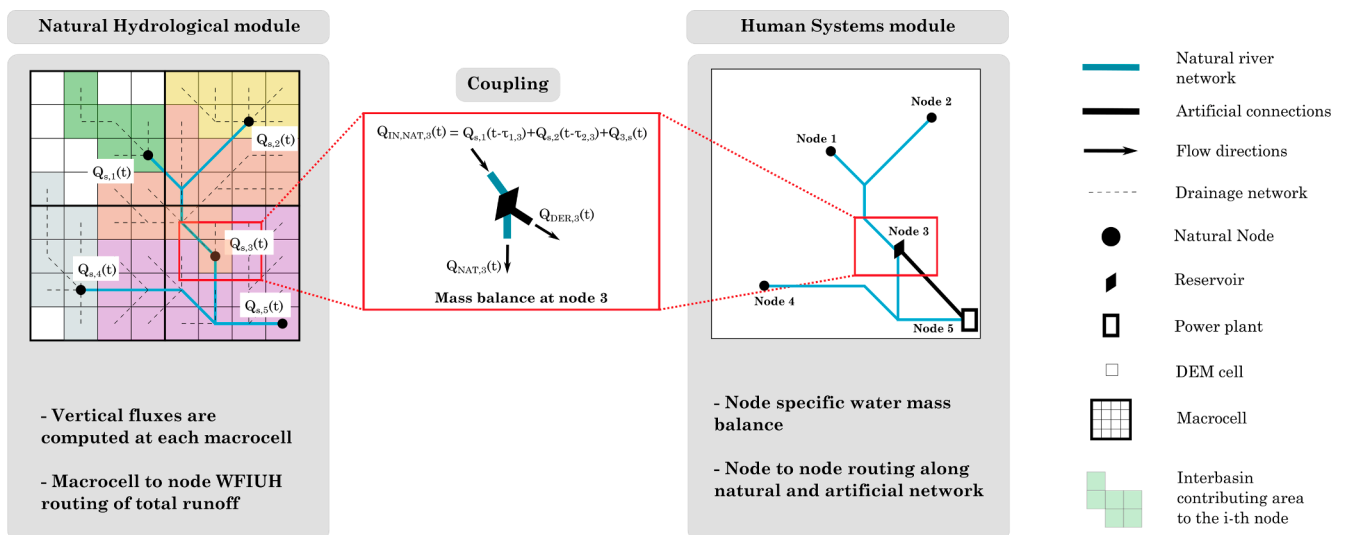


Fig. 1. Schematic representation of HYPERstreamHS hydrological model including its main components and their interaction. The Natural Hydrological module computes vertical fluxes at each cell of the computational grid (macrocell), resulting in total runoff contributions that are then routed to the corresponding downstream node ($Q_{s,i}$ in the left panel). Streamflow contribution from individual interbasins (the different colors identify interbasin areas contributing to each node) and from upstream nodes are then aggregated, in order to provide the input to the water mass balance (central panel) that is applied at each Human Systems node (see Section 2.1.2 for details on the constraints and mass balance applied in each node type). Finally, the outcoming flows from a node are routed along the natural and artificial networks.

penstocks. This allows to fully describe the exchange fluxes between the engineered systems and the river network. These modules are detailed in Avesani et al. (2021).

The water budget (Eq. (1)) at *reservoir* nodes is performed considering all the inflows (ΣQ_{IN}) and the following outflows: derivation to all the uses according to the given schedules (ΣQ_{DER}), release of Minimum Ecological Flow (MEF) (Q_{MEF}) and spilling (Q_{spill}) when the maximum regulation level is exceeded:

$$\frac{dV}{dt} = \Sigma Q_{IN}(t) - \Sigma Q_{DER}(t) - Q_{MEF}(t) - Q_{spill}(t) \quad (1)$$

where V is the volume of water stored in the reservoir, and ΣQ_{DER} is the sum of the flows diverted for multiple water uses, i.e. inflows to the penstocks connected to downstream power houses, although similar considerations can be done for uses other than hydropower, with the possibility that a portion of ΣQ_{DER} is added to precipitation in irrigation areas, in case of an agricultural or multi-uses reservoir. In the present work we do not consider this case, which however can be easily included if needed.

Intake nodes are locations where water is withdrawn from the natural stream network by means of intake structures connected to diversion channels or other conduits. They do not have storage capacity and must obey a *MEF* constraint, similarly to reservoirs, as sketched in the inset (a) of Fig. 2. Mass conservation applied to this type of nodes leads to:

$$\begin{cases} Q_{IN,nat}(t) = Q_{OUT,nat}(t) + Q_{DIV,art}(t) \\ Q_{OUT,art}(t) = Q_{DIV,art}(t) + Q_{IN,art}(t) \end{cases} \quad (2)$$

where the terms of the water budget are distinguished between natural (*nat*) and artificial (*art*) fluxes occurring in the river network and in the engineered components of the system, respectively. In Eq. (2) $Q_{DIV,art}$

varies between zero and the maximum water discharge that the intake can accept. The second Eq. (2) is applied to internal nodes of the engineered system, as for example the nodes along the derivation tunnel represented in the inset (a) of Fig. 2. Intake nodes are also used to model restitution fluxes to the river through a tail race channel (as shown in the inset (b) of Fig. 2). In this case, incoming contributions, natural and from the engineered system, are merged (i.e., summed, according to Eq. (3)) and routed downstream along the stream network.

$$Q_{OUT,nat}(t) = \Sigma Q_{IN,art}(t) + \Sigma Q_{IN,nat}(t) \quad (3)$$

A type-intake node can also be used to model the confluence between conduits, in situations like the one depicted in the inset (c) of Fig. 2. In this case the following continuity equation (Eq. (4)) is applied at the node:

$$Q_{OUT,art}(t) = \Sigma Q_{IN,art}(t) \quad (4)$$

where $Q_{OUT,art}$ and $\Sigma Q_{IN,art}$ are the outflow and sum of the inflow fluxes at the node, respectively.

Finally, *hydropower plant* nodes behave similarly to restitution nodes, routing all incoming flows to the downstream stream network. The HydroPower Production (HPP) at each hydropower system is computed as follows:

$$HPP(t) = \eta \sum_{i=1}^N \rho g Q_{TURB,i}(t) \Delta H_i(t) \quad (5)$$

In Eq. (5) η is the plant's efficiency, which for simplicity is assumed to be the same for all the hydropower plants; $Q_{TURB,i}$ and ΔH_i are the turbined water discharge and the hydraulic head of the i -th power unit, respectively (often for efficiency reasons, and also in case the power house receives water from more than one source, two or more generation units are installed in the same power house). For a storage reservoir

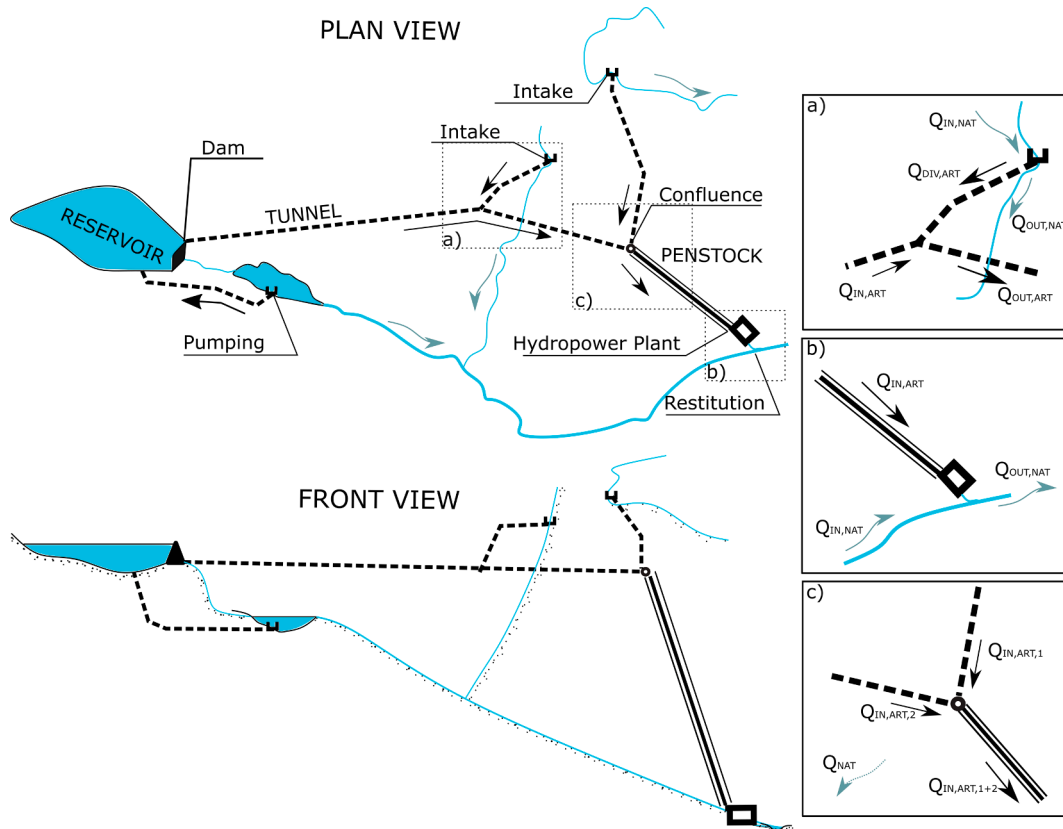


Fig. 2. Sketch of the infrastructures simulated in the Human System module of HYPERstreamHS. Insets to the right detail particular structures modelled by type-intake objects: diversion (a), restitution point (b) and confluence between tunnels (c).

hydropower plant, the head ΔH_i is given by the difference between the reservoir water stage and the level of the nozzle or the water level in the afterbay, depending of the type of turbine. On the other hand, for run-of-the-river power plants, ΔH_i is assumed equal to the gross head of the power plant.

2.2. Data requirements for Natural Hydrological and Human Systems modules

HYPERstreamHS requires gridded input of precipitation, temperature and evapotranspiration at the same time step of the simulation. These inputs can be obtained either by global meteorological datasets or reconstructed by performing interpolation of ground observations with geostatistical tools embedded in the model. Digital Elevation Model (DEM), land-use and land cover maps are also needed to identify the river network and to initialize the spatially varying parameters controlling evapotranspiration and infiltration processes. Daily observed streamflow time series at relevant gauging stations are also needed for calibration and validation of the hydrological model. The data requirements for characterizing the Natural Hydrological module are summarized in Table 1.

Modelling the interactions between the river network and the intertwined hydropower systems requires specific topological and operational data in order to adequately describe the hydraulic infrastructures and reproduce the associated water transfers. Availability of these data is system specific, depending also on the level of industrial secrecy of the producers. In order to make our approach general, we decided to use only data that are publicly available. Unfortunately, very few data are available in the most widely used global datasets, such as Global Reservoir and Dam (GRanD, Lehner et al. (2011)), Global geOreferenced Database of Dams (GOODD, Mulligan et al. (2020)), Future Hydropower Reservoirs and Dams Database (FHReD, Zarfl et al. (2015)), and therefore a specific search in public archives of state agencies or from informative leaflets is unavoidable for a proper model set-up. The full list of topology and operational data needed for an optimal characterization of the systems (by using only public data) is summarized in Table 2.

Furthermore, hydropower production historical data are needed for the validation of the Human System module and for approximating the hydropower production scheme of the individual power plant as described in Section 2.3. Hydropower production time series are publicly available upon request from National Managers of electricity grid, and they are typically provided aggregated in space and time to comply with confidentiality agreements between the public authorities and producers.

We remark that all data used in the present work are publicly available, and this is because our main objective is to develop a methodology that can be used in other contexts, without relying on data collected by the producers, which are often kept confidential. Details about the data used for the case study application are presented in Section 3.

2.3. Hydropower production scheme

In addition to meteorological, geomorphologic and topology data the

Table 1
Data requirements for Natural Hydrological module characterization.

Domain characterization	DEM Hydrologic soil group map Land cover map
Meteorological forcing	Precipitation Dataset (daily) Temperature Dataset (daily) PET Dataset (Hargreaves-Samani)
Hydrological calibration	Streamflow time series at gauging stations

Table 2

Data requirements to fully characterize HS nodes in HYPERstreamHS.

Characteristic	Description	Data type [units]
Reservoir		
x_{res}, y_{res}	Location	CRS: WGS 84-UTM 32N [m]
$Q_{spill,MAX}$	Spillway capacity	[m ³ s ⁻¹]
$V(H)$	Stage-Storage curve	array [m a.s.l. vs. Mm ³]
$h_{min,reg}$	Minimum regulation stage	[m a.s.l.]
$h_{max,reg}$	Maximum regulation stage	[m a.s.l.]
$h_{max,inv}$	Spillway crest elevation	[m a.s.l.]
Q_{SYS}	Hydraulic capacity	[m ³ s ⁻¹]
$Q_{MEF}(t)$	Minimum Ecological Flow	[m ³ s ⁻¹]
Intake		
x_{itk}, y_{itk}	Location	CRS: WGS 84-UTM 32N [m]
$Q_{max,chan}$	Intake capacity	[m ³ s ⁻¹]
$Q_{MEF}(t)$	Minimum Ecological Flow	[m ³ s ⁻¹]
Hydropower Plant		
x_{plt}, y_{plt}	Location	CRS: WGS 84-UTM 32N [m]
H_{plant}	Elevation	[m a.s.l.]
ΔH_{plant}	Gross average head	[m]
P_{ann}	Mean annual production	[MWh/y]
W_{inst}	Installed power	[MW]
η	Plant efficiency	–
Channel		
id_{UP}	Upstream node ID	Node attribute
id_{DOWN}	Downstream node ID	Node attribute
$type_{UP}$	Upstream node type	Node attribute
$type_{DOWN}$	Downstream node type	Node attribute
l	Length	[m]

modelling framework requires the schedule of all the water uses as input. To allow flexibility a schedule is associated to each water use and is provided externally. In particular, hydropower scheduling was inferred from monthly energy production at the province level, which is publicly available, assuming that all the hydropower systems were operated similarly (at this temporal scale). Water use schedules at finer temporal scales could be envisioned in case the information is available. Firstly, the average water discharge taken from the reservoir of a hydropower system is estimated as follows:

$$Q_{AVG,i} = \frac{HPP_{EXP,i}}{\gamma \cdot \eta \cdot \Delta H_i \cdot 24 \cdot 365} \quad (6)$$

where $HPP_{EXP,i}$ is the expected annual production for the i -th power plant, as declared by the company operating the plant and usually computed as long term average, ΔH_i is the gross average head, and η is the total efficiency of the plant. The derived water discharge time series for the single reservoir are then obtained by modulating the average value provided by Eq. (6) according to the following expression:

$$Q_{DER,i}(t) = Q_{AVG,i} k_m(t) \delta_w(t) \phi_e(t) \quad (7)$$

where $k_m = HPP_{aggr,m}/HPP_{aggr,ann}$ is the ratio between the mean production of the m -th month, $HPP_{aggr,m}$, and the long term annual mean, $HPP_{aggr,ann}$, of the available aggregated data of hydropower production, δ_w is a dummy variable introduced to simulate the reduction of production during the weekends and ϕ_e is a function reflecting short-to-medium term variations due to management strategies. Here we used $\phi_e = P_{avg,3}/P_{avg,month}$, where $P_{avg,3}$ is the three-day centered moving average of electricity price and $P_{avg,month}$ is the average price of the month. Moving average is used here to smooth the volatility characterizing the time series of daily electricity prices (see e.g., Demir et al., 2020). The resulting utilization scheme mimics the interplay between variations in hydrology and water uses, the latter influenced by the

electricity market. A similar approach has been adopted by Schaeffli et al. (2007) with a stochastic component that was added to a historical time series with the intent of mimicking the intrinsic variability of the electricity market.

According to Eq. (7) the turbinized water flow is controlled by the parameters k_m , ϕ_e and δ_w , each one addressing a different scale of time variability, with the former varying also in space at the level of the provinces. An example of the resulting utilization scheme is shown in Fig. 3. We observe variations at multiple scales from the monthly scale, chiefly due to seasonal variations of streamflow, to the smaller weekly and daily scales due to fluctuations of the electricity price. Notice the shutoff of production during the weekends when the price of electricity reduces, simulated by setting $\delta_w = 1$ during weekdays, and to 0 in the weekends.

3. Case study and model set-up

3.1. Study area

The Adige river is the second longest Italian river with a contributing area of 10,500 km² at the gauging station of Vó Destro (Fig. 4). The watershed occupies a large portion of the southeastern Alps in a mountain area with elevation ranging from 200 to 3900 m a.s.l. The annual average precipitation ranges from 500 mm in the North-West to 1600 mm in the South (Lutz et al., 2016; Diamantini et al., 2018) with streamflow showing a typical alpine regime with two seasonal maxima, one occurring in spring-summer due to snow and glacier melt, and the other in autumn triggered by cyclonic storms (Chiogna et al., 2016; Lutz et al., 2016; Mallucci et al., 2019).

Fig. 4 shows the natural river network, the superimposed hydropower network, the hydropower plants and the storage reservoirs. Though fragmented, the hydropower network is distributed over the entire river system and exerts a significant impact on streamflow (Majone et al., 2016; Pérez Ciria et al., 2019; Zolezzi et al., 2009).

3.2. Climatic forcing, land cover and geomorphology data

The ADIGE dataset (Mallucci et al., 2019) was used to provide daily air temperature and precipitation forcing to our simulations. The dataset consists of daily readings taken at 244 and 350 gauging stations for precipitation and air temperature respectively, that have been distributed on a 5 × 5 km grid by Ordinary Kriging with External Drift (OKED), adopting terrain elevation as secondary variable (Goovaerts, 1997). Grid resolution was set on the basis of previously published studies conducted in the study region with the same hydrological kernel (Laiti et al., 2018;

Avesani et al., 2021). Moreover, potential evapotranspiration (PET) was computed, according to the Hargreaves-Samani approach (Hargreaves and Samani, 1982) and provided as a gridded input to the model.

Soil elevation and land use information were extracted from the 30 m EUDEM Digital Elevation Model (DEM) and the Corine 2006 dataset (<https://www.eea.europa.eu/publications/COR0-landcover>), respectively. The DEM has been corrected in order to comply with the portions of stream network altered by human intervention, in accordance with the official stream network provided by the Superior Institute for Environmental Protection and Research (ISPRA, available at <http://www.sinanet.isprambiente.it/it/sia-ispra/download-mais/reticolo-idrografico/view>).

3.3. Human Systems in the Adige watershed

Within the catchment operate 39 large hydropower systems with installed power ranging from 5.2 to 230 MW, 22 of which with reservoir (see numbering from 1 to 22 in Fig. 4) with operational volumes ranging from 0.32 to 172 Mm³ (see also Table 3). A rather extensive network of diversion channels with capacity ranging from 0.3 to 203 m³/s is feeding the whole system. The total long term average production of these hydropower systems is of 6609 GWh/y, according to data available from the hydropower companies operating in the river basin, thereby contributing to more than 14% of the annual Italian hydropower production (<https://www.terna.it/it-it/sistemaelettrico/statisticheprevisioni/bilancienergiaelettrica/bilancinazionali.aspx>).

Information concerning topology and operational data of the hydropower systems located in the Adige catchment was collected and structured in a GIS database during the EoCoE-II project (<https://www.eocoe.eu/water-for-energy/>). The main characteristics of both run-of-the-river and storage systems are summarized in Table 3 while the topology of the hydropower network is shown in Fig. 4. Detailed prescriptions for MEF at each water diversion were retrieved from the Public Water Usage Plans of the Trento and Bolzano provinces (available at <http://www.pguap.provincia.tn.it> and <https://ambiente.provincia.bz.it/acqua/piano-generale-utilizzazione-acque-pubbliche.asp>, respectively). The data used to fully characterize HS module in the Adige case study are stored in a public GitHub repository available at <https://github.com/majoneb/HYPERstreamHS>

In the present work plant efficiency η was set constant and equal to 0.8, which is the average of the efficiencies of the hydropower systems for which this information was available (i.e. 12 out of 22 reservoir hydropower systems of the Adige river). This is justified by the similarity in the hydraulic characteristics of the power plants.

3.4. Streamflow and hydropower production time series

Daily streamflow time series at all the relevant gauging stations in the Adige (see Fig. 4) were provided by the Hydrological Offices of Trento (<http://www.floods.it/public/>) and Bolzano (<http://www.provincia.bz.it/hydro/>). These time series are official measurements and are available at a daily or finer time scale, in the 1923–2013 time window, with very few gaps.

Hydropower production data were provided by the Manager of the Italian electricity grid, TERNA (<http://www.terna.it/>). Hydropower production time series are publicly available upon request at a monthly time scale and aggregated by-province; they have been acquired for the 2000–2015 time window with no gaps. Moreover, data are subdivided between small and large hydropower systems (3 MW installed power threshold), in line with the classification commonly adopted in Italy and inherited in the present work, in which only large hydropower plants are taken into account as they contribute for roughly 90% of the total hydropower production. Production data of the Bolzano province can be used directly for model validation since all the hydropower systems of the province are within the upper Adige catchment. This is not the case

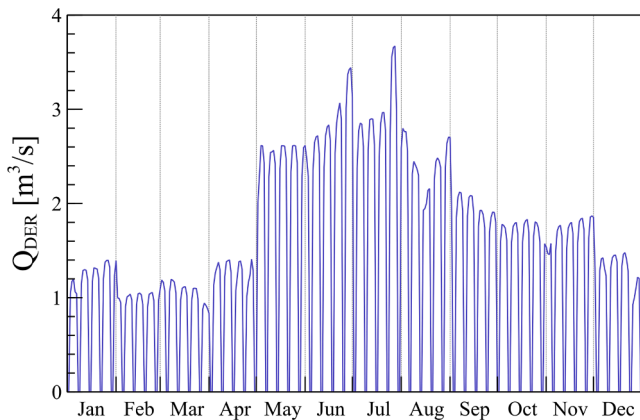


Fig. 3. Example of a water utilization scheme provided by Eq. (7). Turbinized water discharge varies at both monthly and daily scales, the former reflecting streamflow seasonality and the latter influenced by the reduction of the electricity price during the weekends.

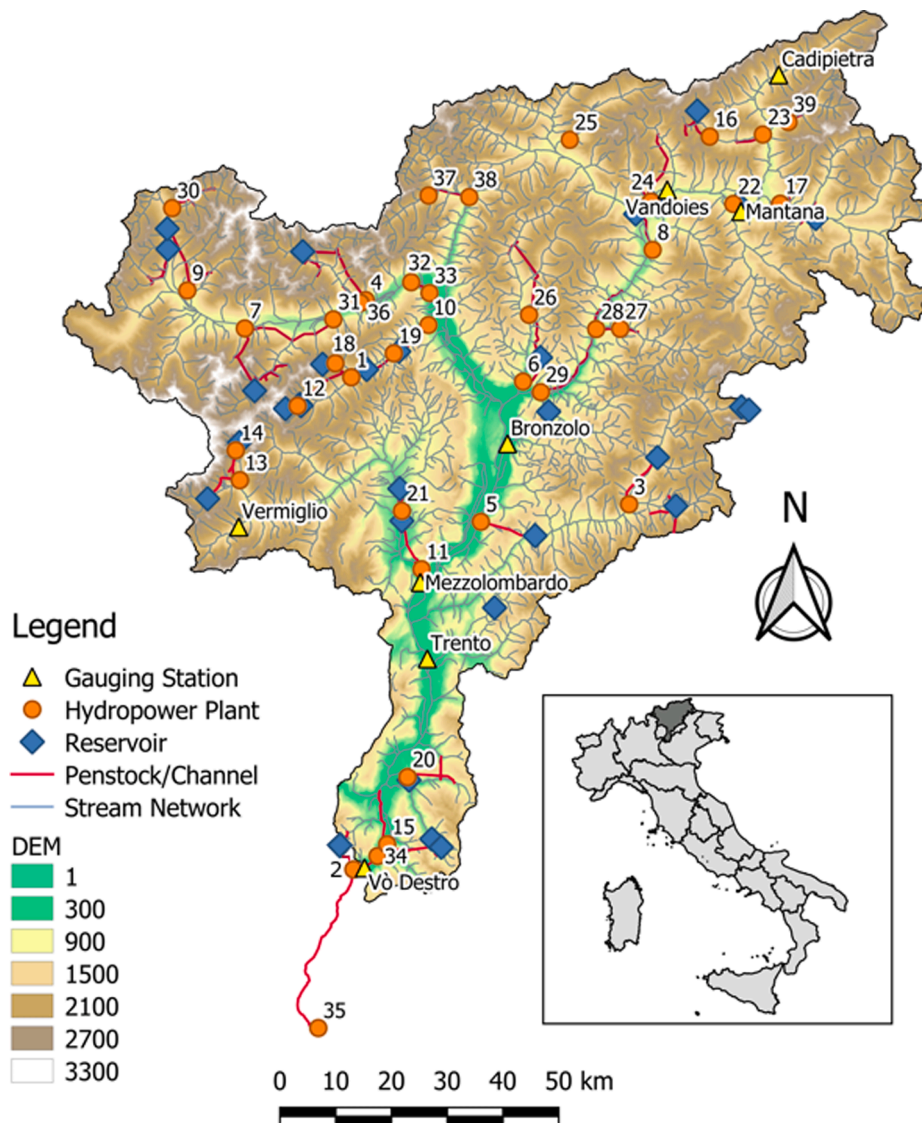


Fig. 4. Location within the Adige watershed of calibration and validation nodes, as well as of the hydropower systems with more than 3MW installed power. Numbering refers to the IDs of the hydropower plants as presented in Table 3. Notice how hydropower systems 2 and 35 have their respective water intakes within the Adige watershed while their tailraces are outside of it.

for the Trento province because only a portion of the hydropower systems is in the (lower) Adige catchment. Consequently, the (observed) production of the lower Adige catchment is estimated by multiplying the production of the Trento province by a factor equal to the fraction of the installed capacity in the Adige catchment with respect to that of the entire province, under the hypothesis that all power plants are operated similarly.

3.5. Hydrological model calibration and validation

HYPERstreamHS was calibrated using the Nash–Sutcliffe (NSE) index (Nash and Sutcliffe, 1970) as objective function and searching the parameters space with the Particle Swarming genetic algorithm (PSO, Kennedy and Eberhart, 1995). As already observed in other works (see, e.g., Bombelli et al., 2019) the common approach of calibrating the model at the catchment outlet does not guarantee good accuracy in the sub-catchments, which are crucial in our simulations because feeding the hydropower systems. To overcome this drawback we adopted a multi-site calibration strategy following the suggestion by Zhang et al. (2008). The model was calibrated by maximizing the global NSE index at the following three gauging stations: Cadipietra (148.8km²), Gadera

(289.9km²) and Vermiglio (79.0km²), all located in undisturbed sub-catchments (see Fig. 4). The calibration was performed in the time window 1989–2013 by using the first two years as spin-off (i.e., they do not contribute to the objective function).

Validation was performed by computing the NSE index at four gauging stations not used in calibration and by comparing the simulated annual energy production provided by Eq. (5) with the measured one. The four gauging stations are: Vandoies (1917km²), Mezzolombardo (1356km²), Bronzolo (7400km²) and Trento (9000km²), as depicted in Fig. 4.

3.6. Simulation Setup

Simulations were performed by using a time step $\Delta t = 1\text{ h}$ to ensure adequate accuracy in routing. Consequently, meteorological data available at a daily time step were scaled accordingly, by assuming a uniform distribution of precipitation and evapotranspiration at the sub-daily scale and a constant temperature equal to the daily mean. The resulting streamflows were then aggregated at the daily scale before computing the NSE index. To emphasize the benefits of including a

Table 3

List of the large hydropower systems operating in the Adige catchment. Systems are distinguished between storage reservoirs (R) and run-of-the-river hydropower systems (RoR).

ID	Plant Name	Type	Installed Power [MW]	Connected Reservoir	Active Storage [Mm ³]
1	Santa Valpurga	R	47.20	Fontana Bianca	1.27
2	Avio	R	5.20	Pra da Stua	1.43
3	Predazzo	R	15.00	Pezze di Moena	0.36
4	Naturno	R	230.00	Vernago	43.00
5	San Floriano	R	195.00	Stramentizzo	10.01
6	Sant' Antonio	R	90.00	Val d'Auna	0.36
7	Lasa	R	63.00	Gioveretto	19.01
8	Bressanone	R	124.00	Rio Pusteria	1.61
9	Glorenza	R	107.00	San Valentino	116.11
10	Lana	R	120.00	Alborelo	3.04
11	Mezzocorona	R	62.96	Mollaro	0.69
12	Fontana Bianca	R	10.50	Lago Verde	6.71
13	Cogolo	R	58.00	Pian Palu	12.55
14	Malga Mare	R	12.00	Careser	15.02
15	Maso Corona	R	40.00	Speccheri	2.24
16	Lappago	R	29.84	Neves	14.37
17	Brunico	R	42.00	Monguelfo	6.07
18	Pracomune	R	42.00	Quaira d. Miniera	12.26
19	San Pancrazio	R	34.85	Zoccolo	33.34
20	San Colombano	R	26.00	San Colombano	7.95
21	Taio	R	105.00	Santa Giustina	172.00
22	Kniepass	R	8.25	Kniepass	0.32
23	Molini	RoR	16.52	–	–
24	Rio Pusteria	RoR	15.00	–	–
25	Val di Vizze	RoR	24.90	–	–
26	Sarentino	RoR	24.41	–	–
27	Premesa	RoR	8.20	–	–
28	Ponte Gardena	RoR	14.48	–	–
29	Cardano	RoR	165.00	–	–
30	Curon Venosta	RoR	12.50	–	–
31	Castelbello	RoR	87.00	–	–
32	Tel	RoR	32.00	–	–
33	Marlengo	RoR	43.60	–	–
34	Ala	RoR	38.00	–	–
35	Bussolengo	RoR	48.00	–	–
36	Senales	RoR	6.40	–	–
37	Moso	RoR	13.00	–	–
38	San Leonardo	RoR	26.00	–	–
39	Campo Tures	RoR	18.00	–	–

suitable representation of hydropower systems' topology and operating rules, four configurations were considered, each one with the hydropower systems represented by using a different level of detail. The adopted simplifications are described here with reference to the sketch shown in Fig. 5:

- **FULL**: this configuration simulates the interaction between natural stream network and hydropower systems with fully detailed topology and reservoir operating rules (see Fig. 5a);
- **NAT**: this is the fully natural condition with all hydraulic infrastructures removed. Therefore, only natural streamflows are computed in this case, with no flow being diverted for hydropower uses (see Fig. 5b). Of course in this case no energy is produced;
- **QMAX**: this configuration includes all the elements of the hydropower system such as the diversion channels, conveyance intakes, tunnels and penstocks. However, reservoir operation rules were simplified, assuming that hydropower plants are always operated at their maximum hydraulic capacity, only obeying mandatory constraints, i.e., minimum and maximum storage capacity, with priority given to the release of *MEF*. Under these conditions Eq. (7) reduces to

$Q_{DER,i}(t) = Q_{SYS,i}$, where $Q_{SYS,i}$ is the hydraulic capacity of the turbines of the i -th power plant (as shown in Fig. 5c);

- **RES**: in this case, storage reservoir operating schemes were implemented with the maximum possible detail (as explained in Section 2.3), but conveyance intakes were neglected, thereby assuming the reservoir as the only water source for the connected generation units. In case of run-of-the-river systems only the main intake was considered. In the Adige watershed only 5 systems were affected by this simplification, whose impact on hydropower production is however worth analysing, given their large capacity. The impact of this modification is exemplified in Fig. 5d, where the contribution of the conveyance intakes is removed from the water discharge delivered to the hydropower plant.

4. Results and Discussion

4.1. Relevance of Human Systems towards streamflow representation

The multi-site calibration of HYPERstreamHS, performed as detailed in Section 3.5 by using the gauging stations of Cadiapietra, Gadera and Vermiglio as reference, produced an overall NSE of 0.63, which can be considered as satisfactory. The model was then validated by comparing the simulated with the measured streamflows at four gauging stations downstream the previous ones and not used for calibration. The streamflow at these stations is altered to a various degree by hydropower and therefore the performance varies according to the adopted configuration as shown in Table 4. Considering the three gauging stations of Vandoies, Bronzolo and Trento, which are mildly impacted by hydropower, the NSE coefficients are larger than the global NSE obtained in calibration. This is an encouraging result and shows that HYPERstreamHS provides a good representation of the hydrological system. The Mezzolombardo gauging station is highly impacted by hydropower (see the discussion later) and although the NSE increases progressively as the hydraulic infrastructures are better detailed its maximum value is below 0.5, which is the lower limit for considering the simulations as satisfactorily (see e.g., Moriasi et al., 2007). In all cases an improvement in the representation of the hydraulic system leads to an increase, though in some cases marginal, of NSE in validation. This shows that including into the modelling effort the hydraulic infrastructures is informative. Similar conclusions were drawn by Dang et al. (2020).

NAT and QMAX configurations produce similar results, since in the latter hydropower systems are always operated at their maximum capacity with reservoirs dramatically reducing their storage. Indeed, in this situation, water is stored only when inflow exceeds the hydraulic capacity (i.e., the maximum water discharge that the power plant can convey to the turbines). On the other hand, also RES and FULL configurations exhibit a similar behavior and this can be attributed to the fact that RES configuration differs from FULL only in 5 systems out of 22 (IDs 1, 4, 9, 13, 26 in Table 3), thereby the impact of a different water use schedule in these systems is hardly noticeable at the validation sites. Consequently, for the sake of clarity, Fig. 6 depicts observed and simulated streamflows for the NAT and FULL configurations, which represent the two extreme cases of ignoring the presence of the hydraulic infrastructures and representing them to the maximum possible level of detail allowed by publicly available data, as discussed in Sections 2.2 and 3.3.

As expected the proper representation of the hydraulic infrastructures is important during low flow periods (from November to March), when hydropower releases affect significantly streamflow timing and magnitude, as confirmed by visual inspection of the flow duration curves depicted in right panel of Fig. 6. On the other hand, no appreciable differences are observed between NAT and FULL configurations during high flow periods (from May to October), because of the cutoff introduced by hydraulic capacity of the hydropower system. Furthermore, the difference between NAT and FULL configurations attenuates as the distance between the gauging station and the intake or

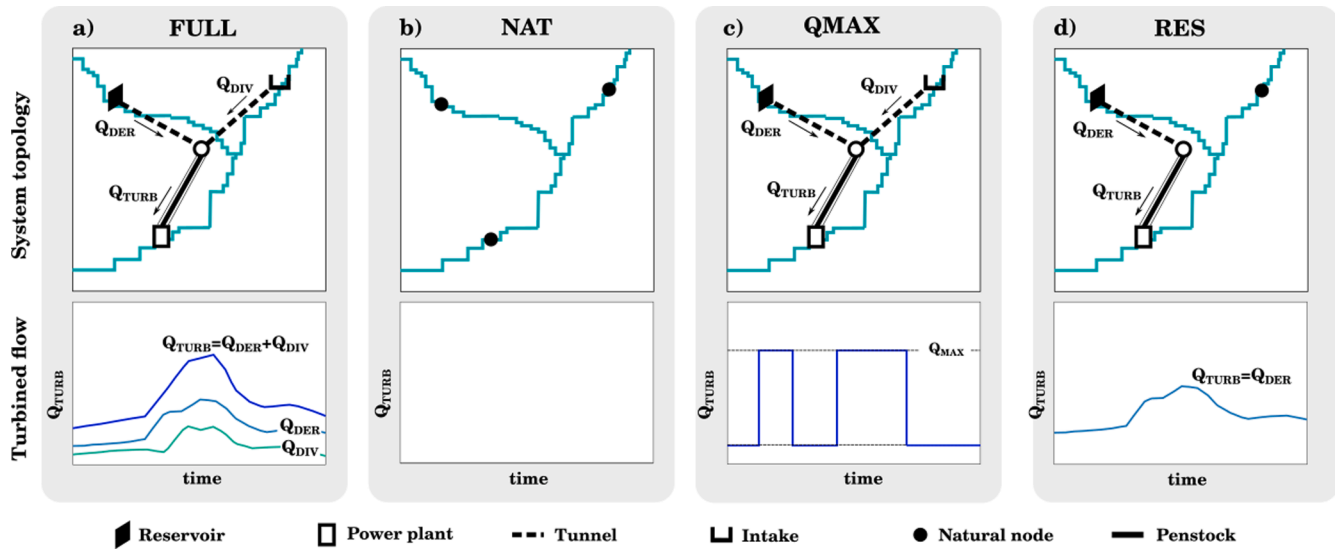


Fig. 5. Schematic representation of the four configurations in terms of hydropower systems' topology and reservoir operating rules.

Table 4

NSE values at validation sites. The introduction of HS module in the simulation improved the NSE at downstream nodes, demonstrating that reproducing the hydraulic systems and their functioning into the hydrological model is informative.

STATION	NSE _{NAT}	NSE _{QMAX}	NSE _{RES}	NSE _{FULL}
Vandoies	0.68	0.66	0.68	0.70
Mezzolombardo	0.14	0.09	0.29	0.34
Bronzolo	0.77	0.77	0.77	0.79
Trento	0.73	0.73	0.77	0.77
AVERAGE	0.58	0.56	0.63	0.65

restitution points of a hydropower system increases. This is the consequence of the reduction of the ratio between the turbined water discharge and streamflow along the river network and away from the hydropower plant. For example, Vandoies, Bronzolo, and Trento gauging stations are located sufficiently far from the closest upstream hydropower system and exhibit the typical seasonal streamflow variability, with small variations and attenuated oscillations during the low flow periods (subplots a), c) and d) in Fig. 6). Conversely, the Mezzolombardo gauging station (see Fig. 4) is located immediately downstream (2km) of the large Mezzocorona hydropower plant (ID 11 in Fig. 4 with a hydraulic capacity of $66 \text{ m}^3 \text{ s}^{-1}$), which dramatically affects the otherwise lower natural streamflows (mean annual value of $\sim 20 \text{ m}^3 \text{ s}^{-1}$ upstream of the system): despite some inaccuracies due to the limited knowledge of reservoir operating rules, the FULL configuration clearly provides the more realistic representation of streamflow, as opposed to the NAT configuration (subplot b) in Fig. 6). From the above considerations it can be concluded that, especially during seasons in which hydropower releases constitute a large share of streamflows (i.e., low flow periods) the benefit of including a detailed modelling of hydropower systems is significant for a proper representation of streamflow alterations.

The impact on streamflow alterations of the three configurations described above was investigated by analyzing the time series of the normalized difference between the streamflow in the presence and in the absence of the hydraulic infrastructures:

$$R_{Q,i}^{\text{conf}}(t) = (Q_i^{\text{conf}}(t) - Q_i^{\text{NAT}}(t)) / Q_i^{\text{NAT}}(t) \quad (8)$$

where $Q_i^{\text{conf}}(t)$ is the daily streamflow computed at node i under the given configuration of the hydraulic infrastructures (with *conf* being

either FULL, RES or QMAX), and $Q_i^{\text{NAT}}(t)$ is the daily streamflow computed at the same node under the natural (NAT) configuration. Mean ($\mu_{R,i}^{\text{conf}} = \frac{1}{n} \sum_{t=1}^n R_{Q,i}^{\text{conf}}(t)$), where n is the number of time steps, and standard deviation ($\sigma_{R,i}^{\text{conf}} = \sqrt{\frac{1}{n} \sum_{t=1}^n [R_{Q,i}^{\text{conf}}(t) - \mu_{R,i}^{\text{conf}}]^2}$) of the normalized residual time series (Eq. (8)) are shown in Fig. 7 left and right columns, respectively. This Figure visualizes in an intuitive manner the most relevant alterations and their spatial pattern.

In the FULL configuration the larger alterations with respect to natural conditions are at reservoir nodes (see full rombi in Fig. 7a) since only MEF and overtop water discharge during flooding feed the channel immediately downstream the impoundment (as detailed in Section 2.1.2). Positive alterations (i.e. streamflow higher than in natural conditions) are observed downstream the restitution of the power plants (blue triangles in Fig. 7a) receiving contribution from outside the catchment, i.e. from catchments not belonging to their contributing area. QMAX and FULL show similar streamflow alterations (Figs. 7c and 7a), given that both elaborate the same annual water volume, though with a different timing. This latter consideration is valid also for the RES configuration, with the exception of the nodes belonging to the five systems (identified by black rectangles in Fig. 7e) that were topologically simplified in the RES configuration. In this case no alterations (i.e. $\mu_{R,i}^{\text{RES}} = 0$) are observed at the nodes where conveyance intakes are deactivated (white dots in Fig. 7e within the black rectangles). However, significant alterations, slightly smaller than in the FULL configuration, are observed at the corresponding nodes of the power plants.

An indicator of alterations in streamflow timing occurring at the daily time scale is the standard deviation of the normalized residual time series (Eq. (8)) shown in the right column of Fig. 7. In the FULL configuration (Fig. 7b) the largest deviations from the natural regime are observed at the hydropower plants connected to large storage reservoirs (see red triangles in Fig. 7b), as a consequence of a changing (in time) hydropower production. The reason of the reduced (with respect to the FULL configuration) standard deviation, $\sigma_{R,i}^{\text{QMAX}}$, observed in Fig. 7d for the QMAX configuration can be identified in the simplification introduced in the reservoir management rules (see Section 3.6), which indeed cause reservoir hydropower systems to be managed similarly to run-of-the-river systems. The effects of an unrealistic hydropower schedule such as that introduced by the QMAX configuration will be further discussed in Section 4.3. Alteration of streamflow timing under RES configuration exhibits a similar pattern as in the FULL configuration with the exception of the nodes belonging to the five

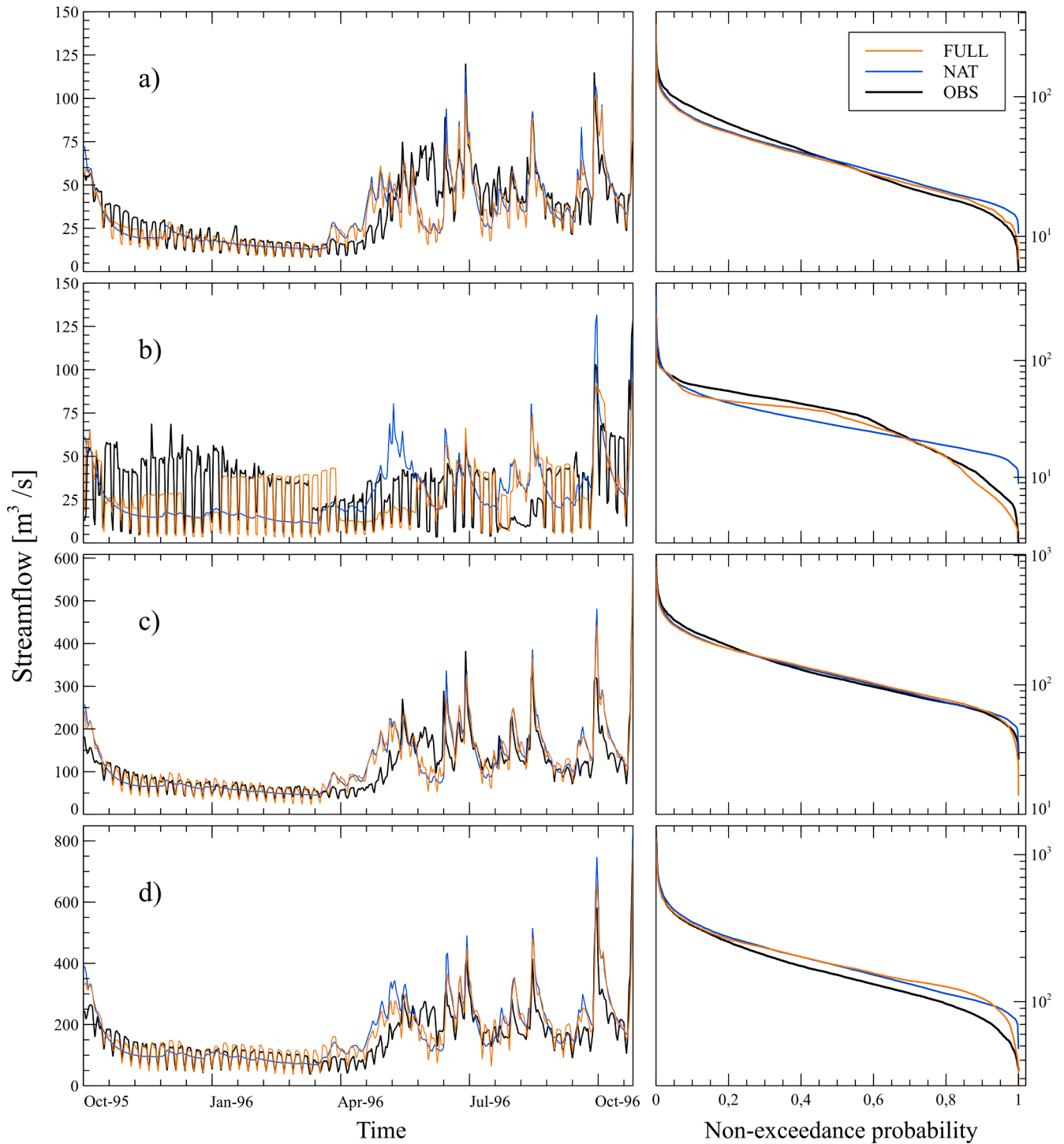


Fig. 6. Comparison between observed and simulated streamflow time series (left column) and flow duration curves (right column) at the validation sites: a) Vandoies, b) Mezzolombardo, c) Bronzolo and d) Trento stream gauging stations. To better showcase the effect of hydropower activities, which introduce periodic oscillations, streamflow is shown only for one hydrological year starting from October 1995, while the FDCs represent the entire simulation period 1991–2013.

systems highlighted in Fig. 7f, where the introduced topological simplification leads to small to negligible variations (i.e. $\sigma_{R,i}^{RES} = 0$) with respect to the reference NAT configuration.

4.2. Impact of customary approximations on hydropower production

The simulated energy production of the Adige catchment in the time window 2000–2013 was compared with the observed one, computed as the sum of the entire production of the province of Bolzano and the

portion of the Trento province pertaining to the Adige watershed, as described in Section 3.4. In particular, Fig. 8 shows the comparison between modelled and observed hydropower production for the configurations described in Section 3.6 at a monthly time scale, with the exception of NAT where by definition modelling of human systems is not performed. The observed and simulated mean annual productions are also summarized in Table 5 where the hydropower systems are grouped into reservoir and run-of-the-river systems.

The FULL configuration provided the better reproduction of average

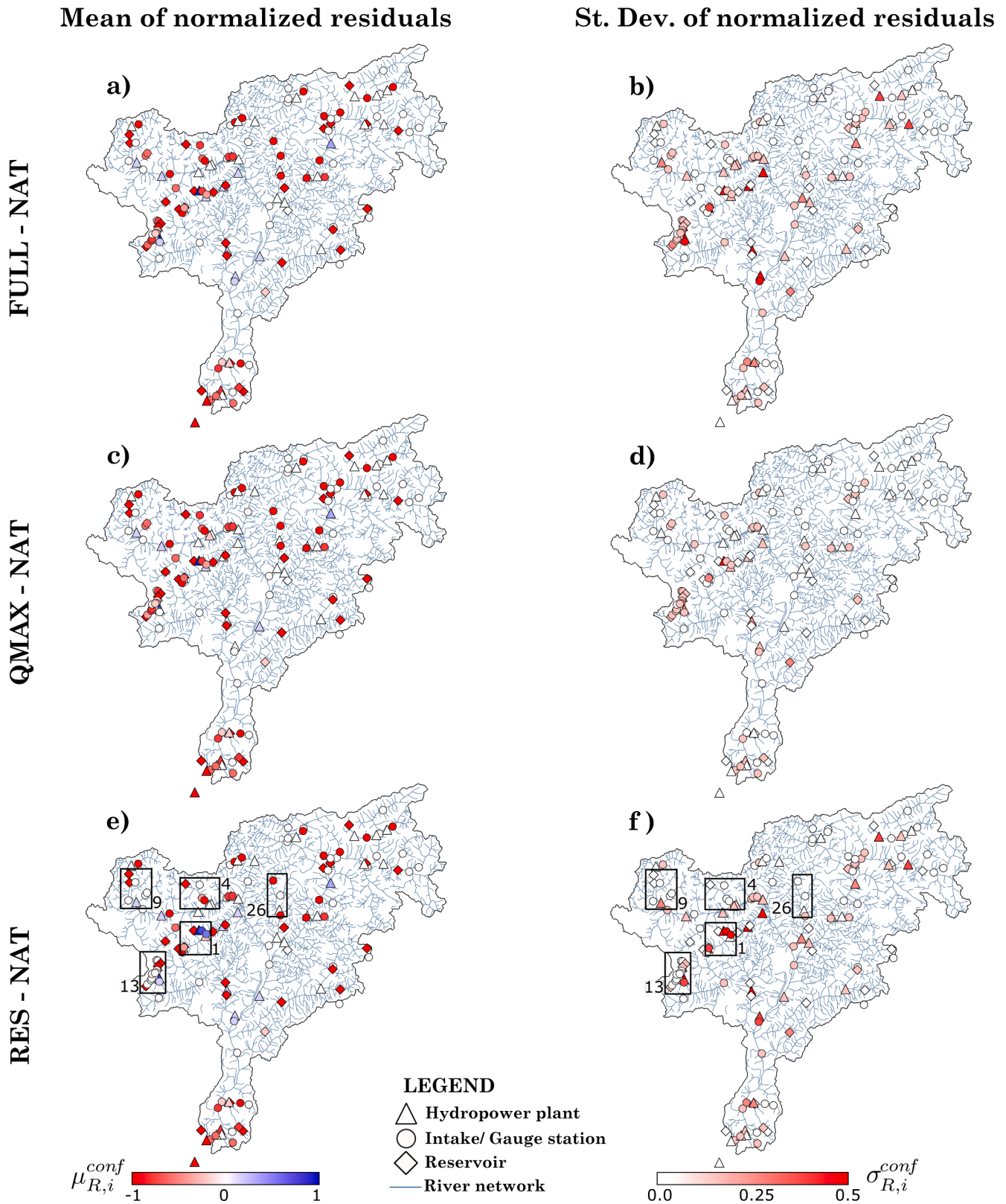


Fig. 7. Analysis of the time series of normalized streamflow differences with respect to the natural streamflow obtained by applying HYPERstreamHS after removing the hydraulic infrastructures. Three utilization scenarios are considered: FULL, QMAX and RES. The left column shows the mean of the normalized streamflow differences at each node, while the right column shows their standard deviation. The hydropower systems highlighted in the rectangular frames of the two bottom panels represent those affected by the simplification introduced in the RES configuration: their numbering refers to the ID presented in [Table 3](#).

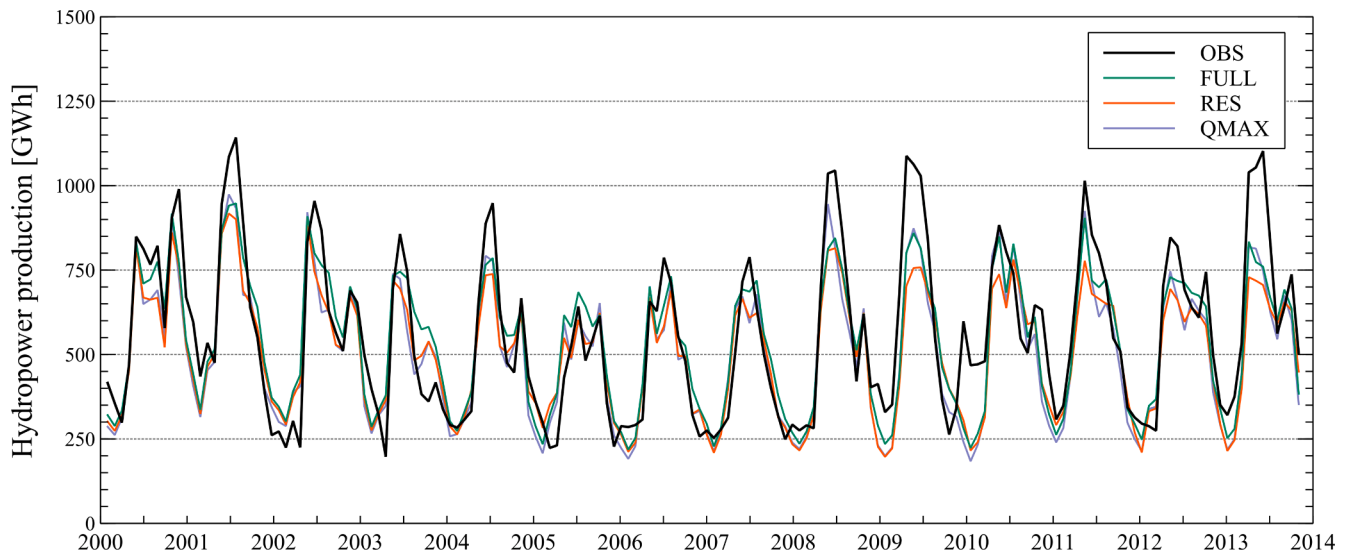


Fig. 8. Simulated and observed monthly hydropower production of the Adige catchment in the timeframe 2000–2013.

Table 5

Comparison of observed and simulated mean annual hydropower production (expressed in GWh/y) over the 2000–2013 time window for each configuration.

	OBS		QMAX		RES		FULL	
	HPP		HPP	%	HPP	%	HPP	%
Total	6717		6043	−10.0	6061	−9.8	6449	−4.0
Storage reservoir	3510		3031	−13.7	3024	−13.9	3306	−5.8
Run-of-the-river	3207		3012	−6.1	3037	−5.3	3143	−2.0

annual hydropower production, with a small difference of 4% due to the imperfect reconstruction of the unknown operational schedule and, to a minor extent, to errors in simulating streamflow entering the reservoirs and at the withdrawal points. On the other hand, QMAX and RES configurations introduce a bias in the representation of hydropower systems, leading to larger errors in the modelled hydropower production. Generally, the errors are smaller for run-of-the-river systems, with a minimum of 2% in the FULL configuration.

Larger deviations in the hydropower production at run-of-the-river systems are indeed observed for QMAX and RES configurations, highlighting that imperfect reconstruction of the operational schedule in storage reservoirs also significantly affects streamflow timing at downstream locations where run-of-the-river plants are located. We consider the high accuracy of the FULL configuration in reproducing historical hydropower production data a significant achievement of the present work. Indeed, existing studies compare different scenarios, either in terms of water usage policies or climate change impacts (see e.g., Meng et al., 2020; Bejarano et al., 2019; Gaudard et al., 2013), but they do not validate the hydropower modelling framework under historical conditions. In our opinion, model validation is a necessary step to avoid possibly biased interpretation of scenario runs. In the ensuing section we provide additional evidence on how the simplified configurations RES and QMAX introduce bias in hydropower production modelling.

4.3. Effects of simplified reservoir operation modelling

We start by evaluating more in detail the effects of the QMAX configuration, which assumes that the storage hydropower systems of the catchment operate at their maximum capacity when the amount of water in their reservoirs is enough to sustain at least one day of production and shut off when it becomes smaller. This simplification is commonly adopted in large scale impact assessment studies (see e.g., Turner et al., 2017; Wagner et al., 2016), as detailed information on

reservoir operation is often hard to obtain. As shown in Table 5, the simulation performed with the QMAX configuration underestimates the total hydropower production more than the other two configurations (RES and FULL). The impact of this assumption is exemplified in Fig. 9, which compares the evolution in time of the water stage in the Gioveretto reservoir under both the QMAX and FULL configurations.

Under the QMAX configuration the reservoir is most of the time at its minimum level (zero utilizable water volume) and therefore the hydropower plant operates most of the time as a run-of-the-river system at the minimum head. This occurs because in the QMAX configuration the water flow withdrawn from the reservoir Q_{DER} is larger than the mean annual water inflow $Q_{IN,AVG}$ and therefore the reservoir is predominantly in low storage conditions. As a consequence, the production reduces because of the lower head, despite the turbined water volume is roughly the same.

The simulated reservoir water stage in the QMAX configuration is, nevertheless, unrealistic. Large reservoirs usually perform seasonal regulation of the water storage, as is the case in the simulation performed under the FULL configuration (see Fig. 9). It should be noticed that a correct timing of hydropower production is important for a proper evaluation of the ecological impact of hydropower systems. In fact, hydropower production may adversely affect reservoir aquatic ecosystems due to internal oscillation of the water stage which, if of large

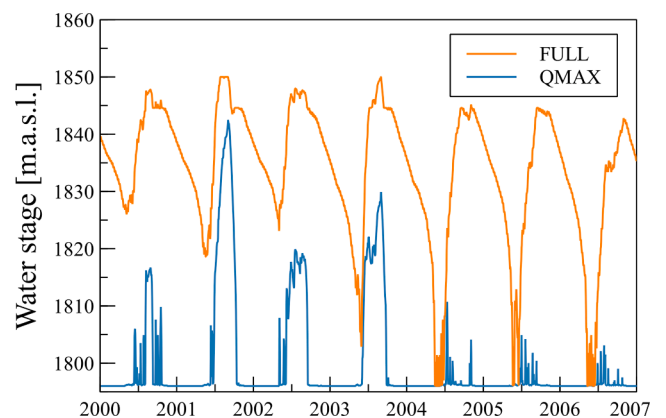


Fig. 9. Water stage time series of the Gioveretto reservoir in the 2000–2006 time window. The QMAX configuration causes a reduction in the average reservoir water level, as opposed to the FULL configuration, obtained from the elaboration of the data provided by TERN, which respects seasonality.

amplitude, may impair the riparian buffer (see e.g., Yang et al., 2018; Renofalt et al., 2010; Jager and Smith, 2008). Similarly, hydropowering may significantly affect freshwater ecosystems downstream the restitution (see e.g., Larsen et al., 2021; Finch et al., 2015; Hall et al., 2015; Bruno et al., 2013). Under this perspective, a realistic and accurate modelling of timing and magnitude of streamflow alterations due to hydropower operation is of deemed importance. From the economical point of view, the cost of these alterations, due to the loss of ecosystem services, should be compared with the increased revenue due to a larger production or a larger share of production in periods with high electricity prices and the reduction of CO₂ emissions. On the other hand, simplifications in the hydropower schedule may lead to inaccuracies in the evaluation of the impacts on the ecosystems (see e.g., Vigiak et al., 2018). Similar conditions to those observed at Gioveretto are observed in the other simulated reservoirs (result not shown here), though the modelled production decreases more in systems in which the head created by the impoundment is a larger fraction of the total head.

4.3.1. Impacts of uncertainty in the hydraulic capacity

Operational rules for reservoirs are often not disclosed by the hydropower companies for not providing advantages to competitors in the same electricity market. Therefore, with the hydraulic capacity as the only information available, large scale studies are conducted by assuming that reservoir hydropower systems are always operated at their hydraulic capacity $Q_{SYS,i}$ with i indicating the hydropower system ($i = 1, \dots, 22$, in our work consistently with Fig. 4 and Table 3). However, this information may be known with uncertainty as well, particularly when the study refers to a large number of hydropower plants. To evaluate the effect of knowing Q_{SYS} with uncertainty we considered two additional configurations with Q_{DER} constant in time (as in the QMAX configuration) and equal to $Q_{DER,i} = k Q_{SYS,i}$, with $i = 1, \dots, 22$ and $k = 0.8$ and 1.2 , respectively. Hereafter, the former configuration is called QMAX_{0.8} and the latter QMAX_{1.2}. Given the relatively small deviation from system capacity Q_{SYS} , the efficiency η is maintained constant and equal to 0.8 .

For the purposes of this analysis, three indicators were computed for each hydropower system. The first indicator is the ratio $I_H(i) = \Delta H(i)/H_{sys}(i)$ between the maximum oscillation, $\Delta H(i)$ of the reservoir level

and the mean total head $H_{sys}(i)$, given by the difference between the elevation of the reservoir center of mass (at the maximum operational level) and the nozzle, or the tailrace, depending on the type of installed turbine. The second indicator, $R_C(i) = V_{OP}(i)/Q_{IN,AVG}(i)$ is the ratio between the operational volume $V_{OP}(i)$ (see Table 3) and the mean annual inflow $Q_{IN,AVG}(i)$. This indicator is equal to the number of days needed to fill the reservoir with a constant inflow $Q_{IN,AVG}(i)$ in the absence of utilization and starting from the minimum level, and it represents the regulation capacity (RC) of the reservoir. In addition, the variation of the modelled hydropower production with respect to the FULL configuration is computed as follows: $\Delta_{PROD}(i) = (HPP_{conf}(i) - HPP_{FULL}(i))/HPP_{FULL}(i)$, where $HPP_{conf}(i)$ is the hydropower production in the selected configuration (i.e., QMAX_{0.8}, QMAX and QMAX_{1.2}) and $HPP_{FULL}(i)$ that of the reference (FULL) configuration.

Results of this analysis are summarised in Fig. 10 in which each column represents one of the 22 storage hydropower systems of the Adige catchment. Systems with $I_H < 7$ (from 1 to 12) do not show significant reductions of the production with respect to the FULL configuration, irrespective to the configuration considered (either QMAX and its two variations described above). This result was expected given the predominance of the geodetic head over the head created by the impoundment, as reflected in the relatively small I_H of these systems. On the other hand, the losses of hydropower production increase with I_H , due to the fact that reservoir oscillations, ΔH , are a significant fraction of the total head. Similarly to QMAX, both QMAX_{0.8} and QMAX_{1.2} configurations reduce the annual production with respect to the FULL configuration (i.e. $\Delta_{PROD} < 0$). The lowest reduction is obtained with the configuration QMAX_{0.8} for most of the systems (i.e., 1,2,4,7,9,10,11,12,13,14,15,16,17,18,19,20,21), however for the systems number 3, 5, 6, 8 and 22 the smallest loss of production is obtained with the configuration QMAX_{1.2}. While the reduction of the loss when the configuration QMAX_{0.8} is used was expected because of the higher simulated average reservoir level with respect to the configuration QMAX, the lowest reduction obtained with the configuration QMAX_{1.2} is counter-intuitive. The explanation is in the low regulation capacity of these reservoirs, all having $R_C < 1$, with the exception of hydropower system number 5. When $R_C < 1$ the reservoir is rapidly filled and the loss of production is proportional to the spilled water volume, which is

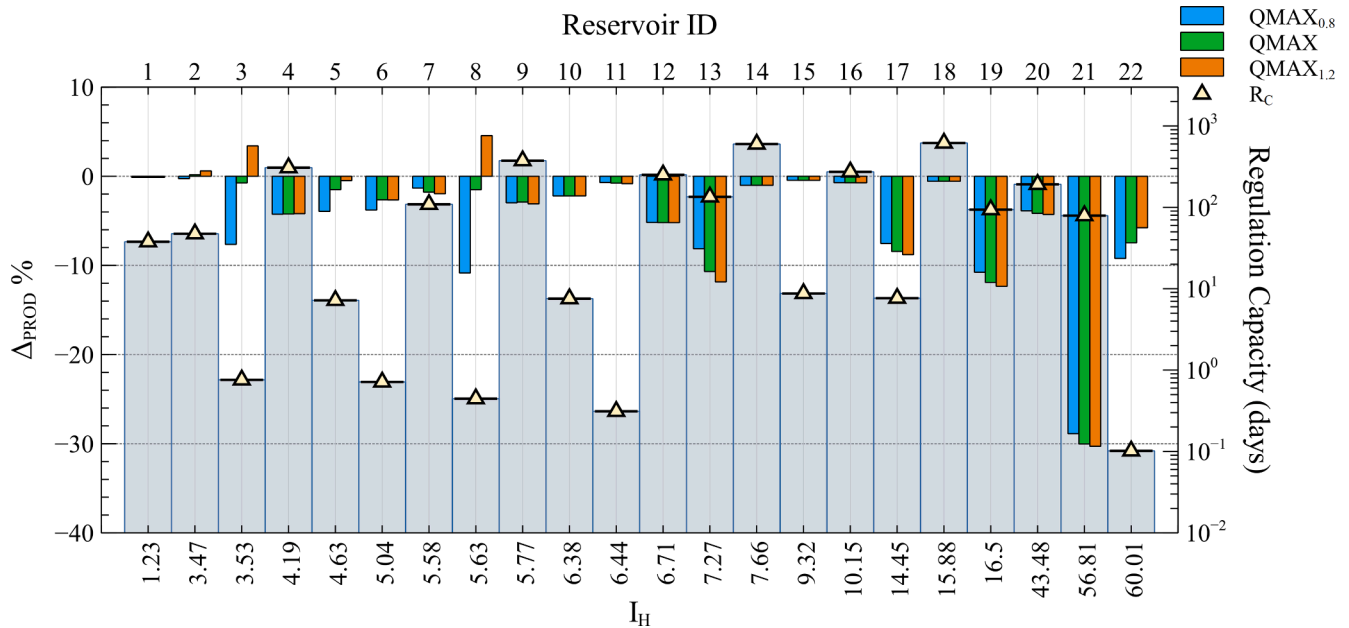


Fig. 10. Effects of incorrect estimation of hydraulic capacity in simplified approaches. Colored bar charts depict the variation in hydropower production Δ_{PROD} for the QMAX_{0.8} (blue), QMAX (green) and QMAX_{1.2} (orange) configurations. Regulation capacity R_C is shown with a grey bar for each system, while the I_H indicator is reported below the horizontal axis.

smaller when Q_{DER} is larger, thereby with the configuration $QMAX_{1,2}$. In the case of system number 5, despite the regulation capacity not usually being a constraint, spilling occurred during some of the extreme high-flow seasons and thus configuration $QMAX_{1,2}$ converted most of the excess flows in hydropower production.

This analysis shows that even when operational schedule is unknown performing the simulation with the QMAX configuration, or a similar one, produces good estimates of the annual energy production. However, simulations lose accuracy for specific hydropower systems with a reservoir whose maximum oscillation is a significant portion of the head. Notably, the system presenting the second largest I_H (i.e., the S. Giustina reservoir connected to the Taio plant, see also Table 3) exhibits a loss of 30% in the annual production.

4.4. Effects of simplified network topology

In the RES configuration only primary water sources, such as the reservoir or the main intake in the run-of-the-river hydropower systems, were included (see Fig. 5d), thereby neglecting the contribution of the conveyance intakes. As a result, natural streamflow was not affected by conveyance intakes ($Q_{DIV,art}(t) = 0$ in Eq. (2)), and turbined volumes were underestimated. This approximation is common in studies at regional, or larger, scales because the technical information needed to simulate conveyance intakes is rarely included into large scale datasets accessible online. In addition to the analysis of the difference between the RES and FULL configurations, we considered a modified configuration, named RES + QMAX, which adds the simplifications in reservoir management (QMAX configuration) to those related to system topology (RES), with the aim to verify if and how these two assumptions interact and influence the accuracy of the modelled hydropower production. Only 5 out of 39 large hydropower systems in the Adige watershed include conveyance intakes and were therefore relevant to this analysis. The percentage contributing area associated to the conveyance intake and I_H indicator of these hydropower systems are shown in Table 6, together with their simulated mean annual production under the different aforementioned configurations.

As expected in all hydropower systems the RES configuration leads to a smaller production than the reference FULL configuration, because of the water volume lost by neglecting the conveyance intakes, which is not compensated by a larger use of the water stored in the reservoir. The production loss is proportional to the drainage area of the conveyance intakes and increases further under the RES + QMAX configuration, except for Sarentino, which is a run-of-the-river power plant operating in conditions similar to QMAX fed by a small impoundment with negligible oscillations ($I_H \simeq 0$). The further loss observed in the combined configuration RES + QMAX is roughly proportional to the structural parameter I_H : this is expected because in systems with high I_H hydropower production is sensitive to changes in the impoundment elevation.

This analysis highlights that despite performing well at the aggregate scale, the RES configuration introduced significant biases in the simulated hydropower production of the systems with conveyance intakes

(see Table 6). Similarly, streamflow is strongly affected by the simplifications introduced in the RES configuration. Both aspects indeed represent a fundamental piece of information for local and regional studies that attempt to analyze competing water uses (La Jeunesse et al., 2016; Majone et al., 2012; Rasanen et al., 2017; Zeng et al., 2017) or to develop sustainable water use policies under a changing climate (see e.g., Grizzetti et al., 2017; Winemiller et al., 2016). Although open source reservoir datasets, such as GRanD (Lehner et al., 2011), GOODD (Mulligan et al., 2020), FHReD (Zarfl et al., 2015), represent a valuable source of information for large scale assessments of reservoir functioning and impacts, those datasets do not include data concerning conveyance intakes nor they provide information about the connected hydropower plants and their operational schedules. Our simulations showed that more comprehensive datasets providing detailed information about hydropower systems and their network topology are a valuable piece of information that should not be disregarded, though difficult to achieve.

5. Conclusions

We analyzed the effects on modelled streamflow and hydropower production of different levels of approximation used to represent the hydropower systems in a hydrological model. A distributed hydrological model (HYPERstreamHS) was first calibrated by using the data of three gauging stations in headwater catchments not influenced by hydropower and other significant water uses. The validation of the modelling framework was then performed by comparing simulations extended to the entire Adige watershed, conducted with the most detailed representation of hydraulic infrastructures that publicly available data allow to achieve (FULL configuration), with historical time series of measured streamflow and hydropower production data.

The FULL configuration was then assumed as reference and compared with three additional simplified configurations typically adopted in large-scale hydrological modelling to make data collection more affordable, RES, QMAX and NAT (assuming the latter as reference for the natural conditions of the watershed). The reference configuration (FULL) provided a very good representation of total hydropower production of the Adige river: at the annual scale the difference with the measured production was only of -4% . Differences of the order of -10% were observed with the other configurations. All configurations including the hydropower systems improved the streamflow representation (i.e., produced higher NSE indexes at the selected stream gauges) in validation with respect to the NAT configuration, thereby confirming the advantage to include, though in an approximate manner, hydraulic infrastructures into hydrological modelling.

Streamflow alterations at the modelling nodes were analyzed by comparing the three hydropower configurations (i.e., FULL, RES and QMAX) with the natural configuration (NAT). Spatial patterns of streamflow alteration magnitude are similar in the three hydropower configurations (Fig. 7a, c, e). The largest increase in streamflow variability, epitomized by the standard deviation of the normalized residuals, is observed for the FULL configuration at the hydropower plants

Table 6

Mean annual simulated HPP for the simplified RES and RES + QMAX configurations in the five hydropower systems characterized by the presence of conveyance water intakes. The Table also presents the percentage contributing area draining at the conveyance water intakes (CI Area), I_H indicator, along with the percentage variations in hydropower production ($\Delta\%$) with respect to the FULL configuration.

Power Plant	Characteristics		FULL HPP	RES		RES + QMAX	
	CI Area	I_H		HPP	$\Delta\%$	HPP	$\Delta\%$
	[%]	/	[GWh/y]	[GWh/y]	[%]	[GWh/y]	[%]
Cogolo	22	7.27	95.43	77.35	-18.95	69.35	-27.33
Glorenza	34	5.77	202.98	162.11	-20.13	156.71	-22.80
Naturno	40	4.19	214.24	136.87	-36.11	130.33	-39.17
Sarentino	46	$\simeq 0$	63.79	31.66	-50.37	31.66	-50.37
S. Valpurga	35	1.23	41.57	19.41	-53.31	19.17	-53.89

connected with large reservoirs, due the relevant hydraulic capacity of the power plant which is typically higher than the mean natural streamflow. Compared to FULL, QMAX configuration shows a lower increase of streamflow variability due to the simplifications introduced in reservoir management. RES configuration shows results similar to FULL with the exception of nodes in which topological simplifications were introduced. Performance analysis of the QMAX configuration at the reservoir scale showed that this approach is acceptable in terms of average annual production, although its performances deteriorate significantly for reservoirs whose oscillations are a relevant portion of the total head of the system, resulting in differences up to 30% in annual production: in these cases, making realistic assumptions of the production schedule substantially improved the reliability of the predictions. In all cases, despite good estimates of the annual production, modelled reservoir levels do not exhibit seasonal patterns, as it would otherwise be expected. The five systems simplified by the RES configuration showed a remarkable reduction of modelled hydropower production, as the main water sources (reservoirs or main intakes) were not able to compensate for the missing flux provided by the conveyance intakes, thereby causing an underestimation up to 53% of hydropower production. This latter result highlights how a detailed conceptual model and an accurate representation of hydraulic infrastructures is a crucial part of the modelling endeavour, often more important than capturing the operational schedule, which is rarely available. Finally, results show that biases in the RES and QMAX configurations do not compensate, rather they accumulate in a non-linear manner (see Table 6).

In the present work we showed that hydrological modelling in catchments with streamflow altered by hydropower, or other water uses, can benefit from including explicitly the functioning (in terms of water transfers) of hydraulic infrastructures into the hydrological model. Given that technical information concerning these hydraulic infrastructures is often lacking or incomplete and difficult to obtain, we developed and tested a modelling approach that relies solely on publicly available information. The comparison with commonly adopted simplifications showed that an accurate search for publicly available data, more than commonly done, is worth the investment of the financial resources and time required to perform it; the reward being chiefly in a more accurate modelling of streamflow and hydropower production for the hydropower systems of the catchment. The proposed framework is also useful to guide modelling of hydropower production at the regional and national scales.

Credit authorship contribution statement

Andrea Galletti: Writing - original draft, Investigation, Methodology, Software, Visualization. **Diego Avesani:** Software, Visualization, Writing - review & editing. **Alberto Bellin:** Writing - review & editing, Conceptualization, Methodology, Supervision. **Bruno Majone:** Writing - review & editing, Conceptualization, Methodology, Supervision, Funding acquisition.

Declaration of Competing Interest

The authors declare that they have no known competing financial interests or personal relationships that could have appeared to influence the work reported in this paper.

Acknowledgments

This research received financial support by the Energy oriented Centre of Excellence (EoCoE-II), GA number 824158, funded within the Horizon2020 framework of the European Union, and by the project "Seasonal Hydrological-Econometric forecasting for hydropower optimization (SHE)" funded within the Call for projects "Research Südtirol/Alto Adige" 2019 Autonomous Province of Bozen/Bolzano - South Tyrol. This research has been also supported by the Italian Ministry of

Education, University and Research (MIUR) under the Departments of Excellence, grant L.232/2016. Streamflow data were provided by the Hydrographic Office of the Autonomous Province of Bolzano (www.provincia.bz.it/hydro) and by the Ufficio Dighe of the Autonomous Province of Trento (www.floods.it). Information on storage reservoirs was retrieved from the Italian Registry of Dams (RID, <http://dgdighe.mit.gov.it>), managed by the Italian Ministry of Infrastructures and Transportation.

References

- Akpınar, A., 2013. The contribution of hydropower in meeting electric energy needs: the case of turkey. *Renewable Energy* 51, 206–219 <http://www.sciencedirect.com/science/article/pii/S0960148112006209>.
- Anghileri, D., Botter, M., Castelletti, A., Weigt, H., Burlando, P., 2018. A comparative assessment of the impact of climate change and energy policies on alpine hydropower. *Water Resour. Res.* 54 (11), 9144–9161 <https://agupubs.onlinelibrary.wiley.com/doi/abs/10.1029/2017WR022289>.
- Avesani, D., Galletti, A., Piccolroaz, S., Bellin, A., Majone, B., 2021. A dual-layer mpi continuous large-scale hydrological model including human systems. *Environ. Modell. Software* 139, 105003.
- Barton, J.P., Infield, D.G., June 2004. Energy storage and its use with intermittent renewable energy. *IEEE Trans. Energy Convers.* 19 (2), 441–448.
- Bejarano, M., Sordo-Ward, A., Gabriel-Martin, I., Garrote, L., 2019. Tradeoff between economic and environmental costs and benefits of hydropower production at run-of-river-diversion schemes under different environmental flows scenarios. *J. Hydrol.* 572, 790–804.
- Bellin, A., Majone, B., Cainelli, O., Alberici, D., Villa, F., 2016. A continuous coupled hydrological and water resources management model. *Environ. Modell. Software* 75, 176–192 <http://www.sciencedirect.com/science/article/pii/S1364815215300712>.
- Beven, K., Binley, A., 1992. The future of distributed models: model calibration and uncertainty prediction. *Hydrol. Process.* 6 (3), 279–298 <https://onlinelibrary.wiley.com/doi/abs/10.1002/hyp.3360060305>.
- Bieber, N., Ker, J.H., Wang, X., Triantafyllidis, C., van Dam, K.H., Koppelaar, R.H., Shah, N., 2018. Sustainable planning of the energy-water-food nexus using decision making tools. *Energy Policy* 113, 584–607.
- Bombelli, G.M., Soncini, A., Bianchi, A., Bocchiola, D., 2019. Potentially modified hydropower production under climate change in the Italian Alps. *Hydrol. Process.* 33 (17), 2355–2372 <https://onlinelibrary.wiley.com/doi/abs/10.1002/hyp.13473>.
- Bruno, M.C., Siviglia, A., Carolli, M., Maiolini, B., 2013. Multiple drift responses of benthic invertebrates to interacting hydropeaking and thermopeaking waves. *Ecohydrology* 6 (4), 511–522.
- Chiogna, G., Majone, B., Cano Paoli, K., Diamantini, E., Stella, E., Mallucci, S., Lencioni, S., Zandonai, F., Bellin, A., 2016. A review of hydrological and chemical stressors in the Adige catchment and its ecological status. *Sci. Total Environ.* 540, 429–443. <https://doi.org/10.1016/j.scitotenv.2015.06.149>.
- Dang, T., Chowdhury, A.K., Galelli, S., 2020. On the representation of water reservoir storage and operations in large-scale hydrological models: implications on model parameterization and climate change impact assessments. *Hydrol. Earth Syst. Sci.* 24, 397–416.
- Demir, S., Mincev, K., Kok, K., Paterakis, N.G., 2020. Introducing technical indicators to electricity price forecasting: a feature engineering study for linear, ensemble, and deep machine learning models. *Appl. Sci.* 10 (1).
- Destouni, G., Jaramillo, F., Prieto, C., 2013. Hydroclimatic shifts driven by human water use for food and energy production. *Nature Climate Change* 3, 213–217.
- Diamantini, E., Lutz, S.R., Mallucci, S., Majone, B., Merz, R., Bellin, A., 2018. Driver detection of water quality trends in three large European river basins. *Sci. Total Environ.* 612, 49–62 <http://www.sciencedirect.com/science/article/pii/S004896971732171X>.
- Faticchi, S., Rimkus, S., Burlando, P., Bordoy, R., Molnar, P., 2015. High-resolution distributed analysis of climate and anthropogenic changes on the hydrology of an alpine catchment. *J. Hydrol.* 525, 362–382.
- Finch, C., Pine III, W.E., Limburg, K.E., 2015. Do hydropeaking flows alter juvenile fish growth rates? a test with juvenile humpback chub in the Colorado river. *River Res. Appl.* 31 (2), 156–164.
- Finger, D., Heinrich, G., Gobiet, A., Bauder, A., 2012. Projections of future water resources and their uncertainty in a glacierized catchment in the Swiss Alps and the subsequent effects on hydropower production during the 21st century. *Water Resour. Res.* 48 (2) <https://agupubs.onlinelibrary.wiley.com/doi/abs/10.1029/2011WR010733>.
- Gabbud, C., Lane, S.N., 2016. Ecosystem impacts of alpine water intakes for hydropower: the challenge of sediment management. *WIREs Water* 3 (1), 41–61 <https://onlinelibrary.wiley.com/doi/abs/10.1002/wat2.1124>.
- Gaudard, L., Gilli, M., Romero, F., 2013. Climate change impacts on hydropower management. *Water Resour. Manage.* 27.
- Goovaerts, P., 1997. *Geostatistics for Natural Resource Evaluation*. Vol. 42. Ch. 8, pp. 388–390.
- Grizzetti, B., Pistocchi, A., Liqueste, C., Udias, A., Bouraoui, F., Bund, W., 2017. Human pressures and ecological status of European rivers. *Sci. Rep.* 7.
- Guo, X., Hu, T., Wu, C., Zhang, T., Lv, Y., 2013. Multi-objective optimization of the proposed multi-reservoir operating policy using improved NSPSO. *Water Resour. Manage.* 27.

- Gupta, H.V., Kling, H., Yilmaz, K.K., Martinez, G.F., 2009. Decomposition of the mean squared error and nse performance criteria: implications for improving hydrological modelling. *J. Hydrol.* 377 (1), 80–91 <http://www.sciencedirect.com/science/article/pii/S0022169409004843>.
- Hall Jr., R.O., Yackulic, C.B., Kennedy, T.A., Yard, M.D., Rosi-Marshall, E.J., Voichick, N., Behn, K.E., 2015. Turbidity, light, temperature, and hydropeaking control primary productivity in the colorado river, grand canyon. *Limnol. Oceanogr.* 60 (2), 512–526.
- Hargreaves, G., Samani, Z., 1982. Estimating potential evapotranspiration. *J. Irrig. Drainage Division – ASCE* 108, 225–230.
- IEA, 2018. International energy agency report on renewable energies. <https://www.iea.org/renewables2018/>, accessed: 2019-Aug-02.
- Jager, H.I., Smith, B.T., 2008. Sustainable reservoir operation: can we generate hydropower and preserve ecosystem values? *River Res. Appl.* 24 (3), 340–352.
- Kennedy, J., Eberhart, R., Nov 1995. Particle swarm optimization. In: *Proceedings of ICNN'95 – International Conference on Neural Networks*. Vol. 4. pp. 1942–1948 vol 4.
- La Jeunesse, I., Cirelli, C., Aubin, D., Larrue, C., Sellami, H., Afifi, S., Bellin, A., Benabdallah, S., Bird, D.N., Deidda, R., Dettori, M., Engin, G., Herrmann, F., Ludwig, R., Mabrouk, B., Majone, B., Paniconi, C., Soddu, A., 2016. Is climate change a threat for water uses in the Mediterranean region? Results from a survey at local scale. *Sci. Total Environ.* 543, 981–996. <https://doi.org/10.1016/j.scitotenv.2015.04.062>.
- Laiti, L., Mallucci, S., Piccolroaz, S., Bellin, A., Zardi, D., Fiori, A., Nikulin, G., Majone, B., 2018. Testing the hydrological coherence of high-resolution gridded precipitation and temperature data sets. *Water Resour. Res.* 54 (3), 1999–2016.
- Larsen, S., Majone, B., Zulian, P., Stella, E., Bellin, A., Bruno, M.C., Zolezzi, G., 2021. Combining hydrologic simulations and stream-network models to reveal flow-ecology relationships in a large alpine catchment. *Water Resour. Res.* 57 (4) <https://doi.org/10.1029/2020WR028496> e2020WR028496.
- Lehner, B., Liemann, C.R., Revenga, C., Vörösmarty, C., Fekete, B., Crouzet, P., Döll, P., Endejan, M., Frenken, K., Magome, J., Nilsson, C., Robertson, J.C., Rödel, R., Sindorf, N., Wisser, D., 2011. High-resolution mapping of the world's reservoirs and dams for sustainable river-flow management. *Front. Ecol. Environ.* 9 (9), 494–502 <https://esajournals.onlinelibrary.wiley.com/doi/abs/10.1890/100125>.
- Lutz, S.R., Mallucci, S., Diamantini, E., Majone, B., Bellin, A., Merz, R., 2016. Hydroclimatic and water quality trends across three mediterranean river basins. *Sci. Total Environ.* 571, 1392–1406 <http://www.sciencedirect.com/science/article/pii/S0048969716315480>.
- Majone, B., Bertagnoli, A., Bellin, A., 2010. A non-linear runoff generation model in small alpine catchments. *J. Hydrol.* 385 (1), 300–312 <http://www.sciencedirect.com/science/article/pii/S0022169410001228>.
- Majone, B., Bovolo, C.I., Bellin, A., Blenkinsop, S., Fowler, H.J., 2012. Modeling the impacts of future climate change on water resources for the gallego river basin (spain). *Water Resour. Res.* 48 (1) <https://agupubs.onlinelibrary.wiley.com/doi/abs/10.1029/2011WR010985>.
- Majone, B., Villa, F., Deidda, R., Bellin, A., 2016. Impact of climate change and water use policies on hydropower potential in the south-eastern Alpine region. *Sci. Total Environ.* 543, 965–980. <https://doi.org/10.1016/j.scitotenv.2015.05.009> <http://www.sciencedirect.com/science/article/pii/S004896971530067X>.
- Mallucci, S., Majone, B., Bellin, A., 2019. Detection and attribution of hydrological changes in a large alpine river basin. *J. Hydrol.* 575, 1214–1229 <http://www.sciencedirect.com/science/article/pii/S0022169419305712>.
- Malm Renöfält, B., Jansson, R., Nilsson, C., 2010. 01, Effects of hydropower generation and opportunities for environmental flow management in swedish riverine ecosystems. *Freshw. Biol.* 55, 49–67.
- McKay, M.D., Beckman, R.J., Conover, W.J., 1979. A comparison of three methods for selecting values of input variables in the analysis of output from a computer code. *Technometrics* 21 (2), 239–245 <http://www.jstor.org/stable/1268522>.
- Meng, Y., Liu, J., Leduc, S., Mesfun, S., Kraxner, F., Mao, G., Qi, W., Wang, Z., 2020. Hydropower production benefits more from 1.5 °c than 2 °c climate scenario. *Water Resour. Res.* 56 (5) e2019WR025519.
- Michel, C., Andréassian, V., Perrin, C., 2005. Soil conservation service curve number method: How to mend a wrong soil moisture accounting procedure? *Water Resour. Res.* 41 (2).
- Moriasi, D., Arnold, J., Van Liew, M., Bingner, R., Harmel, R., Veith, T., 2007. Model evaluation guidelines for systematic quantification of accuracy in watershed simulations. In: *Trans. ASABE* 50.
- Mulligan, M., van Soesbergen, A., Saenz, L., 2020. 01, Goodd, a global dataset of more than 38,000 georeferenced dams. *Sci. Data* 7, 31.
- Nash, J., Sutcliffe, J., 1970. River flow forecasting through conceptual models part i – a discussion of principles. *J. Hydrol.* 10 (3), 282–290 <http://www.sciencedirect.com/science/article/pii/0022169470902556>.
- Nazemi, A., Wheeler, H.S., 2015. On inclusion of water resource management in earth system models – part 2: Representation of water supply and allocation and opportunities for improved modeling. *Hydrol. Earth Syst. Sci.* 19 (1), 63–90 <https://www.hydrol-earth-syst-sci.net/19/63/2015/>.
- Nazemi, A., Wheeler, H.S., 2015. On inclusion of water resource management in earth system models; part 1: Problem definition and representation of water demand. *Hydrol. Earth Syst. Sci.* 19 (1), 33–61 <https://www.hydrol-earth-syst-sci.net/19/33/2015/>.
- Pérez Ciria, T., Labat, D., Chiogna, G., 2019. Detection and interpretation of recent and historical streamflow alterations caused by river damming and hydropower production in the adige and inn river basins using continuous, discrete and multiresolution wavelet analysis. *J. Hydrol.* 578.
- Petruzzello, A., Bonacina, L., Marazzi, F., Zaupa, S., Mezzanotte, V., Fornaroli, R., 2021. Effects of high-altitude reservoirs on the structure and function of lotic ecosystems: a case study in Italy. *Hydrobiologia* 848, 1455–1474.
- Piccolroaz, S., Di Lazzaro, M., Zarlinga, A., Majone, B., Bellin, A., Fiori, A., 2016. Hyperstream: a multi-scale framework for streamflow routing in large-scale hydrological model. *Hydrol. Earth Syst. Sci.* 20 (5), 2047–2061 <https://www.hydrol-earth-syst-sci.net/20/2047/2016/>.
- Piccolroaz, S., Majone, B., Palmieri, F., Cassiani, G., Bellin, A., 2015. On the use of spatially distributed, time-lapse microgravity surveys to inform hydrological modeling. *Water Resour. Res.* 51 (9), 7270–7288.
- Rasanen, T.A., Someth, P., Lauri, H., Koponen, J., Sarkkula, J., Kumm, M., 2017. Observed river discharge changes due to hydropower operations in the upper mekong basin. *J. Hydrol.* 545, 28–41.
- Renofalt, B.M., Jansson, R., Nilsson, C., 2010. Effects of hydropower generation and opportunities for environmental flow management in swedish riverine ecosystems. *Freshw. Biol.* 55 (1), 49–67.
- Rodríguez-Turbe, I., Rinaldo, A., 1997. Fractal River Basins — chance and self-organization. Cambridge University Press, Cambridge.
- Schaeffli, B., Hingray, B., Musy, A., 2007. Climate change and hydropower production in the swiss alps: quantification of potential impacts and related modelling uncertainties. *Hydrol. Earth Syst. Sci.* 11 (3), 1191–1205 <https://www.hydrol-earth-syst-sci.net/11/1191/2007/>.
- Sharif, H.O., Crow, W., Miller, N., Wood, E., 2007. Multidecadal high-resolution hydrologic modeling of the arkansas-red river basin. *Journal of Hydrometeorology* 8.
- Shrestha, S., Khatiwada, M., Babel, M., Parajuli, K., 2014. Impact of climate change on river flow and hydropower production in kulekhani hydropower project of nepal. *Environ. Processes* 1.
- Simonov, E.A., Nikitina, O.I., Egidarev, E.G., 2019. Freshwater ecosystems versus hydropower development: Environmental assessments and conservation measures in the transboundary amur river basin. *Water* 11 (8) <https://www.mdpi.com/2073-4441/11/8/1570>.
- Smajgl, A., Ward, J., Pluschke, L., 2016. The water-food-energy nexus – realising a new paradigm. *J. Hydrol.* 533, 533–540 <https://www.sciencedirect.com/science/article/pii/S0022169415009816>.
- Tu, M.-Y., Hsu, N.-S., Yeh, W., 2003. Water resour plan man-ASCE, Optimization of reservoir management and operation with hedging rules. *J. Water Resour. Planning Manage.-asce - J* 129.
- Turner, S.W., Hejazi, M., Kim, S.H., Clarke, L., Edmonds, J., 2017. Climate impacts on hydropower and consequences for global electricity supply investment needs. *Energy* 141, 2081–2090 <https://www.sciencedirect.com/science/article/pii/S0360544217319473>.
- Turner, S.W., Ng, J.Y., Galelli, S., 2017. Examining global electricity supply vulnerability to climate change using a high-fidelity hydropower dam model. *Sci. Total Environ.* 590–591, 663–675 <http://www.sciencedirect.com/science/article/pii/S0048969717305272>.
- United Nations, D. o. E., Social Affairs, P.D., 2019. World population prospects 2019: Highlights (st/esa/ser/a/423). https://population.un.org/wpp/Publications/Files/WPP2019_Highlights.pdf, accessed: 2020-Jan-02.
- Vigiak, O., Lutz, S., Mentzafou, A., Chiogna, G., Tuo, Y., Majone, B., Beck, H., de Roo, A., Malagó, B., Bouraoui, F., Kumar, R., Samaniego, L., Merz, R., Gamvroudis, C., Skoulikidis, N., Nikolaidis, N.P., Bellin, A., Acuna, V., Mori, N., Ludwig, R., Pistocchi, A., 2018. Uncertainty of modelled flow regime for flow-ecological assessment in southern europe. *Sci. Total Environ.* 615, 1028–1047.
- Wada, Y., de Graaf, I.E.M., van Beek, L.P.H., 2016. High-resolution modeling of human and climate impacts on global water resources. *J. Adv. Model. Earth Syst.* 8 (2), 735–763.
- Wagner, T., Themeßl, M., Schuppel, A., Gobiet, A., Stigler, H., Birk, S., 2016. 12 Impacts of climate change on stream flow and hydro power generation in the alpine region. *Environ. Earth Sci.* 76, 4.
- Waldman, J., Sharma, S.N., Afshari, S., Fekete, B.M., 2019. Solar-power replacement as a solution for hydropower foregone in us dam removals. *Nature Sustain.* 2, 872–878.
- Wang, G., Fang, Q., Zhang, L., Chen, W., Chen, Z., Hong, H., 2010. Valuing the effects of hydropower development on watershed ecosystem services: Case studies in the jiu-long river watershed, fujian province, china. *Estuarine, Coastal and Shelf Science* 86 (3), 363–368, eMECS8 – Harmonizing catchment and estuary. <https://www.sciencedirect.com/science/article/pii/S0272771409001401>.
- Winemiller, K., McIntyre, P., Castello, L., Fluet-Chouinard, E., Giarrizzo, T., Nam, S., Baird, I., Darwall, W., Lujan, N., Harrison, I., Stiassny, M., Silvano, R., Fitzgerald, D., Pelicice, F., Agostinho, A., Gomes, L., Albert, J., Baran, E., Petre, M., Saenz, L., 2016. 01, Balancing hydropower and biodiversity in the amazon, congo, and mekong. *Science* 351, 128–129.
- Yang, S., Bai, J., Zhao, C., Lou, H., Zhang, C., Guan, Y., Zhang, Y., Wang, Z., Yu, X., 2018. The assessment of the changes of biomass and riparian buffer width in the terminal reservoir under the impact of the south-to-north water diversion project in china. *Ecol. Ind.* 85, 932–943.
- Yu, B., 2017. 05, The ecological damage compensation for hydropower development based on trade-offs in river ecosystem services. *IOP Conf. Ser.: Earth Environ. Sci.* 64, 012047.
- Zarfl, C., Lumsdon, A.E., Berlekamp, J., Tydecks, L., Tockner, K., 2015. A global boom in hydropower dam construction. *Aquat. Sci.* 77, 161–170. <https://doi.org/10.1007/s00027-014-0377-0>.
- Zeng, R., Cai, X., Ringler, C., Zhu, T., Feb 2017. Hydropower versus irrigation—an analysis of global patterns. *Environ. Res. Lett.* 12 (3), 034006.
- Zhang, X., Li, H.-Y., Deng, Z.D., Ringler, C., Gao, Y., Hejazi, M.I., Leung, L.R., 2018. Impacts of climate change, policy and water-energy-food nexus on hydropower

- development. *Renewable Energy* 116, 827–834 <https://www.sciencedirect.com/science/article/pii/S0960148117309928>.
- Zhao, C., Shao, N., Yang, S., Ren, H., Ge, Y., Zhang, Z., Feng, P., Liu, W., 2019. Quantitative assessment of the effects of human activities on phytoplankton communities in lakes and reservoirs. *Sci. Total Environ.* 665, 213–225.
- Zhang, X., Srinivasan, R., Van Liew, M., 2008. Multi-Site Calibration of the SWAT Model for Hydrologic Modeling. *Trans. ASABE* 51. <https://doi.org/10.13031/2013.25407>.
- Zhao, G., Gao, H., Naz, B.S., Kao, S.-C., Voisin, N., 2016. Integrating a reservoir regulation scheme into a spatially distributed hydrological model. *Adv. Water Resour.* 98, 16–31 <http://www.sciencedirect.com/science/article/pii/S0309170816305504>.
- Zierl, B., Bugmann, H., 2005. Global change impacts on hydrological processes in alpine catchments. *Water Resour. Res.* 41 (2).
- Zolezzi, G., Bellin, A., Bruno, M.C., Maiolini, B., Siviglia, A., 2009. Assessing hydrological alterations at multiple temporal scales: Adige river, Italy. *Water Resour. Res.* 45 (12) <https://agupubs.onlinelibrary.wiley.com/doi/abs/10.1029/2008WR007266>.